PRIFYSGOL ABERYSTWYTH UNIVERSITY

Aberystwyth University

Appraising the capability of a land biosphere model as a tool in modelling land surface interactions: results from its validation at selected European ecosystems

North, Matthew; Petropoulos, George; Ireland, Gareth; McCalmont, Jon

DOI:
10.5194/esdd-6-217-2015

Publication date:
2015

Citation for published version (APA):
North, M., Petropoulos, G., Ireland, G., & McCalmont, J. (2015). *Appraising the capability of a land biosphere model as a tool in modelling land surface interactions: results from its validation at selected European ecosystems*. (pp. 217–265). Copernicus Publications. https://doi.org/10.5194/esdd-6-217-2015

General rights
Copyright and moral rights for the publications made accessible in the Aberystwyth Research Portal (the Institutional Repository) are retained by the authors and/or other copyright owners and it is a condition of accessing publications that users recognise and abide by the legal requirements associated with these rights.

• Users may download and print one copy of any publication from the Aberystwyth Research Portal for the purpose of private study or research.
• You may not further distribute the material or use it for any profit-making activity or commercial gain
• You may freely distribute the URL identifying the publication in the Aberystwyth Research Portal

Take down policy
If you believe that this document breaches copyright please contact us providing details, and we will remove access to the work immediately and investigate your claim.

tel: +44 1970 62 2400
email: is@aber.ac.uk

Download date: 09. Jul. 2020

Earth Syst. Dynam. Discuss., 6, 217–265, 2015
www.earth-syst-dynam-discuss.net/6/217/2015/
doi:10.5194/esdd-6-217-2015
© Author(s) 2015. CC Attribution 3.0 License.

Earth System Dynamics
Discussions
Open Access

This discussion paper is/has been under review for the journal Earth System Dynamics (ESD). Please refer to the corresponding final paper in ESD if available.

Appraising the capability of a land biosphere model as a tool in modelling land surface interactions: results from its validation at selected European ecosystems

M. R. North[1], **G. P. Petropoulos**[1], **G. Ireland**[1], **and J. P. McCalmont**[2]

[1]Department of Geography & Earth Sciences, Aberystwyth University, Aberystwyth, SY23 3DB, UK
[2]Institute of Biological, Rural and Environmental Sciences, Aberystwyth University, Aberystwyth, SY23 3EB, UK

Received: 7 January 2015 – Accepted: 12 January 2015 – Published: 9 February 2015

Correspondence to: G. P. Petropoulos (george.petropoulos@aber.ac.uk)

Published by Copernicus Publications on behalf of the European Geosciences Union.

ESDD
6, 217–265, 2015

Appraising the capability of a land biosphere model as a tool in modelling land surface interactions

M. R. North et al.

Title Page
Abstract | Introduction
Conclusions | References
Tables | Figures
◀ | ▶
◀ | ▶
Back | Close
Full Screen / Esc
Printer-friendly Version
Interactive Discussion

Abstract

In this present study the ability of the SimSphere Soil Vegetation Atmosphere Transfer (SVAT) model in estimating key parameters characterising land surface interactions was evaluated. Specifically, SimSphere's performance in predicting Net Radiation (R_{net}), Latent Heat (LE), Sensible Heat (H) and Air Temperature (T_{air}) at 1.3 and 50 m was examined. Model simulations were validated by ground-based measurements of the corresponding parameters for a total of 70 days of the year 2011 from 7 CarboEurope network sites. These included a variety of biomes, environmental and climatic conditions in the models evaluation.

Overall, model performance can largely be described as satisfactory for most of the experimental sites and evaluated parameters. For all model parameters compared, predicted H fluxes consistently obtained the highest agreement to the in-situ data in all ecosystems, with an average RMSD of 55.36 $\mathrm{W\,m^{-2}}$. LE fluxes and R_{net} also agreed well with the in-situ data with RSMDs of 62.75 and 64.65 $\mathrm{W\,m^{-2}}$ respectively. A good agreement between modelled and measured LE and H fluxes was found, especially for smoothed daily flux trends. For both T_{air} 1.3 m and T_{air} 50 m a mean RMSD of 4.14 and 3.54 °C was reported respectively.

This work presents the first all-inclusive evaluation of SimSphere, particularly so in a European setting. Results of this study contribute decisively towards obtaining a better understanding of the model's structure and its correspondence to the real world system. Findings also further establish the model's capability as a useful teaching and research tool in modelling Earth's land surface interactions. This is of considerable importance in the light of the rapidly expanding use of the model worldwide, including ongoing research by various Space Agencies examining its synergistic use with Earth Observation data towards the development of operational products at a global scale.

ESDD

6, 217–265, 2015

CC BY

1 Introduction

Global climate change is currently facilitating large scale changes within the atmosphere, biosphere, geosphere and hydrosphere (Steinhauser et al., 2012). Quantification and management of such changes and a better understanding of the interactions between different components of the Earth system has been identified nowadays as an important and urgent research direction to be addressed within numerous scientific disciplines (Coudert et al., 2008; Petropoulos et al., 2013a). It also serves as essential information for policy makers and the wider global community (IPCC, 2009). Accurate monitoring of water and vegetation stress is now of prominent global concern and it is regarded as a high priority issue within several European Union (EU) frameworks. This is particularly so for communities in water limited environments, or areas which rely on rain fed agriculture, such as some regions in the Mediterranean basin (European Commission, 2009; Amri et al., 2014).

Accurate estimation of energy fluxes and their partitioning has never been more important in the face of increasing climate change (WMO, 2002; ESA, 2014). The terrestrial boundary layer and its vegetation play a critical role in regulating the partitioning of incoming energy (into latent (LE), sensible (H), and ground (G) heat fluxes) and in the land–atmosphere exchange of carbon dioxide (CO_2), and the close relationship between photosynthesis and the energy and water vapour cycles (Prentice et al., 2014). On this basis, the need to develop a thorough understanding of how heat and water fluxes are characterised in different ecosystems is imperative. This is due to the profound contribution these parameters make to various biogeophysical processes at the planetary boundary layer (Feddema et al., 2005). Currently, the physical interactions behind land surface processes are relatively well-documented within the global scientific community. However, there is a need for further research towards improving our understanding of temporal and spatial dynamics of energy and water fluxes (Quintana-Segui et al., 2008) and the complexity of regional energy and water exchanges (Braud et al., 1995). Also, there is a requirement to provide, at increased estimation accuracy,

ESDD
6, 217–265, 2015

CC BY

parameters characterising the energy and water cycles at different observations scales (Anderson et al., 2008; Amri et al., 2014).

Research undertaken to improve our understanding on the representation of land atmosphere interactions has lead to the development and exploration of a wide variety of modelling schemes. Since the 1970's the global scientific community has developed numerous land surface models (LSMs) to assess a multitude of parameters associated with land surface interactions with varying degrees of complexity and applicability (Olchev et al., 2008). LSMs have evolved from simple bucket models without vegetation consideration (e.g. Manabe, 1969) into credible representations of the exchanges of energy, water and carbon dioxide in the soil-vegetation-atmosphere continuum. The use of Soil Vegetation Atmosphere Transfer (SVAT) models represent one of the most common approaches in studying land surface processes and the interactions between the Earth's system components. SVAT models are mathematical representations of vertical "views" of the physical mechanisms controlling energy and mass transfers in the soil-vegetation-atmosphere continuum. Those models are able to provide deterministic estimates of the time course of soil and vegetation state variables at time-steps compatible with the dynamics of atmospheric processes.

Those models have arisen as a convergence of several needs (Petropoulos et al., 2009a), namely: (i) to better understand land/atmosphere boundary transfers, (ii) to investigate how vegetation responds to climate change and (iii) to assess hydrological balances and measure conditions at a given boundary level. One of their main relative advantages, compared to traditional techniques, is the ability to simulate at a fine temporal resolution (often less than 1 h); this subsequently allows simulations to be in satisfactory agreement with the timescale of the physical process being simulated. In addition to this, SVATs comprehensively analyse a large array of parameters associated with the hydrological, radiative and physical domains of the Earth's energy and water cycles. To this end, such models are widely regarded as the most suitable tool to analyse various complex land surface interactions. SVAT models can be employed as "decision making tools" within policy implementation because of their ability to holisti-

ESDD
6, 217–265, 2015

CC BY

cally and accurately assess numerous parameters in past, present, and future environments. Yet, their predictions have an undefined spatial coverage and are limited in their ability to simulate energy and water transfers only within an area representative of their initial parameterisation. Therefore, surface heterogeneity presents itself as a pertinent problem in the application of those models to more fragmented landscapes, where the high levels of internal biophysical variability cannot be fully represented within the model's parameterisation (Oltchev et al., 2002; Falge et al., 2005; Olioso et al., 2005; Samaali et al., 2007). Additionally, SVAT models often require a large amount of input parameters for initialisation. This makes the widespread application and transferability of those models in some cases troublesome. This is because obtaining site specific parameters in remote and data scarce areas is often very difficult (Oltchev et al., 2002). Current research has led to the development of SVATs incorporating sub-grid scale heterogeneity and with improved representation of plant physiological processes. Evidently, the incorporation of these additional processes has further increased the complexity and number of input parameters required to implement such models.

It is important to note, however, that uncertainty is inevitable in any model since it will never be as complex as the reality it portrays (Denti, 2004). As such, the process of validating a mathematical model is an essential step in its development. Generally speaking, the validation of a model consists of determining how well the model performs when comparing its simulated results with those from the real world. Numerous model validation techniques exist; for a comprehensive overview see Bellocchi et al. (2010). A common strategy is to quantitatively compare the model's predictions vs. actual in-situ observations on the basis of various appropriate statistical metrics. Validation techniques are often also implemented over numerous land cover types, helping to further identify how energy and water fluxes are characterised within different ecological settings. Such techniques help develop confidence in the model's ability to be used within these settings and also contribute to our overall understanding on how land cover types characterise local energy and water fluxes (Coudert et al., 2008). Sensitivity analysis (SA) can also be performed as a key component of any

ESDD
6, 217–265, 2015

CC BY

model evaluation, including SVATs. SA utilises mathematical techniques which aim to quantify the relative influence of each input parameter on the model's output variability (Tomlin, 2013; Vanuytrecht et al., 2014). It allows for an objective assessment of model structure and coherence (Petropoulos et al., 2013a; Gan et al., 2014). In addition, Kramer et al. (2002), in an attempt to holistically assess the capability of a model in portraying a real world system, has proposed a set of model assessment criteria, namely: accuracy, generality and realism. Accuracy is described as the "goodness of fit" of a models estimations to in-situ measurements. Generality is described as the applicability of the model in numerous ecosystems. Realism is described as the ability of the model to address relationships between modelled phenomena. It is widely agreed however, that sometimes discrepancies between the modelled and observed datasets can be partly attributed to uncertainty within the observational dataset itself (Denti, 2004; Wang et al., 2004; Verbeeck et al., 2009). Therefore validation attempts not only require a highly accurate observational dataset (Wang et al., 2004), but also a wider understanding of problems associated to equifinality, insensitivity and uncertainty when assessing biophysical models (Verbeeck et al., 2009).

SimSphere is one example of a SVAT model, developed by Carlson and Boland (1978) to increase our understanding of boundary layer processes. Since its original development, the model has diversified and become highly varied in its applicational use (for a comprehensive overview of the model use refer to Petropoulos et al., 2009a). SimSphere's development as a research, educational and training tool is currently expanding within several universities worldwide. Furthermore, its use synergistically with Earth Observation (EO) data is at present being considered by several Space Agencies towards the development of spatio-temporal estimates of evapotranspiration (ET) rates and surface soil moisture (Mo) products at an operational scale globally (Chauhan et al., 2003; ESA STSE, 2012). These investigations have been based around the implementation of a data assimilation technique termed the "triangle" on which SimSphere is used synergistically with EO data (Carlson, 2007; Petropoulos and Carlson, 2011). Furthermore, a variant of this "triangle" approach is already in use in Spain to

ESDD
6, 217–265, 2015

CC BY

deliver an operational product of surface soil moisture at 1 km spatial resolution from the Soil Moisture and Ocean Salinity (SMOS) satellite launched by the European Space Agency (ESA) (Piles et al., 2011).

Thus, it is understandable that it is of primary importance to perform a variety of validatory tests to appraise SimSphere's adequacy and coherence in terms of its ability to realistically represent Earth surface processes. In this respect, a series of SA experiments have already been conducted on SimSphere (Petropoulos et al., 2009b, 2013a, b, 2014a, b). Those studies provided for the first time independent evidence to enhance our understanding of the model's behaviour, coherence and correspondence to what it has been built to simulate. Yet, validation studies performing direct comparisons of model predictions against corresponding in-situ data on the basis of statistical metrics proposed in the classic literature have been scarce and incomprehensive, only performed over a very small range of land use/cover types (e.g. Todhunter and Terjung, 1987; Ross and Oke, 1988). This despite the fact that this type of validation approach is a common strategy in examining the accuracy of model predictions (e.g. Falge et al., 2005; Giertz et al., 2006; Marshall et al., 2013). Given SimSphere's current global expansion, this type of validation is both timely and of fundamental importance in further establishing the model's structure, coherence and representativeness.

With regards to the elements discussed above, this paper investigates the applicability of SimSphere in reproducing a series of observed parameter validations characterising land surface interactions at a total of 7 European ecosystems. The objective was to thoroughly understand the model's ability to simulate, at a local scale, key parameters characterising Earth's energy and water budgets, namely: net Radiation (R_{net}), Latent Heat (LE), Sensible Heat (H), and Air temperature (T_{air}) at 1.3 and 50 m. Model validation is performed through a comparison of the model predictions against corresponding data belonging to CarboEurope, the largest in-situ monitoring network in Europe which provides validated measurements of key micrometeorological parameters.

ESDD
6, 217–265, 2015

2 Model formulation

This work deals with the SimSphere 1-D boundary layer model devoted to the study of energy and mass interactions of the Earth system. Formerly known as the Penn-State University Biosphere–Atmosphere Modeling Scheme (PSUBAMS) (Carlson and Boland, 1978; Lynn and Carlson, 1990), it was considerably modified to its current state by Gillies et al. (1997) and later by Petropoulos et al. (2013c). It is currently maintained and freely distributed by the Department of Geography and Earth Sciences at Aberystwyth University (http://www.aber.ac.uk/simsphere). This section aims at providing an overview of the model architecture, based on the most recent implementation by Gillies et al. (1997).

SimSphere represents various physical processes taking place in a column that extends from the root zone below the soil surface up to a level well above the surface canopy, the top of the surface mixing layer. Essentially, SimSphere is a 1-dimensional two-source SVAT model with a plant component. Three main systems are represented within SimSphere's structure, namely the *physical*, the *vertical* and the *horizontal* layers (Fig. 1). The *physical* components ultimately determine the microclimate conditions in the model and are grouped into three categories, *radiative, atmospheric and hydrological*. The primary forcing of this component is the available clear sky radiant energy reaching the surface or the plant canopy, calculated as a function of sun and earth geometry, atmospheric transmission factors for scattering and absorption, the atmospheric and surface emissivities and surface (including soil and plant) albedos. The *vertical structure* components, effectively correspond to the components of the Planetary Boundary Layer (PBL) which is divided into three layers – a surface mixing layer, a surface of constant flux layer and a surface vegetation or bare soil layer, where the depths of the first layer is somewhat variable with time, growing throughout the day as H flux is added from below. The depth of the constant flux and vegetation layers are set in the model input, although the depth of a bare soil transition (between soil and air) layer is variable in time depending on the wind speed and the surface roughness.

ESDD
6, 217–265, 2015

In addition, the vertical structure also contains a fourth layer, the substrate layer, which refers to the depth of the soil over which heat and water is conducted.

The vegetation component is dormant at night, that is, after radiation sunset. The night-time dynamics for the surface fluxes differ from those during the day time. LE and H fluxes are exchanged between both the ground and foliage, between plant and interplant airspaces through stomatal and cuticular resistances in the leaf (for water vapour) and the air, between soil and the interplant air spaces and between the entire vegetation canopy and the air. A separate component exists for the bare soil fluxes between the surface and the air. Vegetation and soil fluxes merged at the top of the vegetation canopy. Their relative weights depend on the fractional vegetation cover, specified as an input to the model. As such, SimSphere is referred to as a form of two-stream or two-source model. An important factor in controlling, in particular, the partitioning between LE and H is the stomatal resistance component within the vegetation parameterisation settings. SimSphere provides a choice of two stomatal resistance parameterisations, Deardoff (1978) and Carlson and Lynn (1991). The first is inclusive of the stomatal resistance behaviour that is affected by soil, water and sunlight. However, the inability to measure plant hydraulics (a major attributing factor to vegetation transpiration) is seen to be a prominent disadvantage. The second measures stomatal resistance as a function of leaf–atmosphere vapour pressure difference. This is measured by the difference within the mesophyll and epidermal leaf water potentials, as the stomatal resistance is directly proportional to the vapour pressure difference. The main advantage of this parameterisation setting is the ability to analyse the transpiration plateau effect, described in more detail in Carlson et al. (1991). Further details about the model architecture can be found in Gillies (1993).

The processes and interactions simulated by the model are allowed to develop over a 24 h cycle at a chosen time step, starting from a set of initial conditions given in the early morning (at 05:30 LT – local time) with a continuous evolving interaction between soil, plant and atmosphere layers. A large amount of input parameters are required for the model parameterisation, 53 in total, categorised into 7 defined groups; time and location, vegetation, surface, hydrological, meteorological, soil and atmospheric (Table 1). From initialisation, over a 24 h cycle SimSphere assesses the diurnal evolution of more than 30 prognostic variables associated with the radiative, hydrological and atmospheric physical domains. Numerous physical processes are simulated and all parameters are evaluated as a function of time and their diurnal evolution. Outputs of the model include, between others, the surface energy fluxes (LE and H fluxes) below and at the soil surface, around and above the vegetation canopy and the transfer of water in the soil and in the plants. It also simulates the CO_2 (carbon dioxide) flux between the atmosphere and the plants and the surface O_3 (ozone) flux. Several meteorological parameters are also assessed such as the radiometric surface temperature, wind velocity, air temperature, and humidity at various levels in and above the canopy, plus a number of other plant parameters, such as stomatal resistance and leaf water potential.

3 Materials and methods

This section provides a synopsis of the methodology followed in evaluating SimSphere's ability to simulate key parameters characterising land surface interactions. An overview of the main steps included in this process is furnished in Fig. 2.

3.1 In-situ datasets collection

Reliable data is needed to calibrate and evaluate the predictions of any model (Wang et al., 2004). Therefore, in this study, in-situ data from selected sites belonging to the CarboEurope ground monitoring network were obtained. The latter is part of a larger observational network, FLUXNET (Baldocchi et al., 2001), which is currently the largest global network acquiring ancillary information of micro-meteorological flux and a number of ancillary parameters. Once the data reaches FLUXNET, it is quality controlled and gap-filled using techniques described by Papale et al. (2006) and Moffat

Discussion Paper | Discussion Paper | Discussion Paper | Discussion Paper |

ESDD
6, 217–265, 2015

et al. (2007). As a result, the in-situ data can be provided to the end users community at different processing levels.

In this study, SimSphere's ability to provide estimates of key parameters characterising our water and energy balance was evaluated at 7 CarboEurope sites. These sites were representative of different ecosystem types with markedly different site characteristics (Table 2). All available in-situ data for each site was obtained for the year 2011, allowing for a sufficient database for model parameterisation and validation to be developed. All data was acquired from the European Fluxes database Cluster (http://gaia.agraria.unitus.it/). In particular Level 2 data was obtained across all selected sites for consistency. This product includes the originally acquired in-situ measurements from which only the removal of erroneous data caused by obvious instrumentation error has been undertaken. In addition, atmospheric profile (i.e. radiosonde) data were obtained for each site/day by the University of Wyoming (http://weather.uwyo.edu/upperair/sounding.html). This data included the atmospheric profile of temperature, dew point temperature, wind direction, wind speed and atmospheric pressure.

3.2 Validation days selection

Further analysis was implemented to identify the specific days for which SimSphere would be parameterised and validated for each experimental site. Initially, for each site, cloudy days were identified and subsequently excluded from further analysis. Judgment on which days (or time-periods) were cloud-free was based on analysis of the diurnal observation of shortwave incoming solar radiation (Rg). Cloud-free days were flagged as those having smooth and symmetrical Rg curves, a property signifying clear-sky conditions (Carlson et al., 1991).

Subsequently, for the cloud-free days, the energy balance closure (EBC) was evaluated. EBC evaluation has been accepted as a valid method for accuracy assessment of the turbulent fluxes derived from eddy covariance measurements (Wilson et al., 2002; Li et al., 2005).

Evaluation of EBC using the above equation is only directly relevant to the assessment of LE and H fluxes, and not to other scalar fluxes such as CO_2 (e.g. Wilson et al., 2002; Foken et al., 2006). Energy imbalance derived from implementation of the EBC principle has been found to have implications for the way these energy flux measurements should be interpreted, and therefore, on how they should be compared with model simulations (e.g. Twine et al., 2000; Culf et al., 2002).

EBC was evaluated herein principally by performing a regression analysis (e.g. see Wilson and Baldocchi, 2000; Wilson et al., 2002; Oliphant et al., 2004). The linear regression coefficients (slope and intercept) as well as the coefficient of determination (R^2) were calculated from the ordinary least squares (OLS) relationship between the half-hourly estimates of the dependent flux variables ($\mathrm{LE}+H$) and the independently derived available energy ($R_{\mathrm{net}}-G-S$). In addition to this, the Energy Balance Ratio (EBR) was computed by cumulatively summing $R_{\mathrm{net}}-G-S$ and $\mathrm{LE}+H$ from the 30 min mean average surface energy flux components, and then rationing each of the cumulative sums as follows (e.g. Oliphant et al., 2004; Liu et al., 2006):

$$\mathrm{EBR}=\frac{\sum(\mathrm{LE}+H)}{\sum(R_{\mathrm{net}}-G-S)}. \tag{1}$$

This index ranges generally from zero to one, with values closer to one highlighting a satisfactory diurnal energy closure, indicating a good quality of in-situ measurements. All days with poor EBC ($\mathrm{EBR}<0.750$, $\mathrm{slope}<0.85$, $R^2<0.930$) were excluded from further analysis.

Further constraints were subsequently employed to ensure that selected days were of the highest possible quality in terms of in-situ data quality. Firstly, all days selected were within the growing season of April–October; this eliminated the main effects ascribed to the inter-annual variability in vegetation phenology. Secondly, selected simulation days were assessed for atmospherically stable conditions, namely low wind speeds and small available energy (Maayar et al., 2001). Such conditions were identified by the evaluation of the in-situ dataset, where direct measurements of wind speed

ESDD
6, 217–265, 2015

CC BY

and energy flux amplitude and diurnal trend were used as indicators of atmospherically stable conditions. However, it should be noted that for the IT_Ro3 site no in-situ measurements of air temperature were available for August and September. As a result it was not possible to evaluate the model's performance for this period. In the end, a final set of a total of 70 non-consecutive days from the 7 different CarboEurope sites were identified as being suitable to proceed with the SimSphere validation.

3.3 SimSphere parameterisation and implementation

As already stated (Sect. 2), SimSphere has been developed to simulate the various physical processes that take place as a function of time in a column that extends from the root zone below the soil surface up to a level higher than the surface vegetation canopy. In the horizontal domain, SimSphere implicitly refers to a horizontal area of undefined size that can be composed of a mixture of bare soil and vegetation. Thus, it is conceivable that the horizontal scale for the model is defined by the degree to which the model's initial conditions are representative of the horizontal area to be simulated. In theory, this scale should also be used for the validation process. Consequently, SimSphere parameterisation was carried out at the measurement scale of the flux tower observations. That is a function of the area of the fetch around which the tower is built and the footprint of the turbulent flux measurements, representing an area of $\sim 1\,\text{km}^2$ for the test sites as they are relatively homogeneous.

On this basis SimSphere was parameterised to the daily conditions existing at the flux tower for each of the selected days. Initial conditions for T_{air}, humidity, wind velocity and direction soundings were acquired at 06:00 GMT from the University of Wyoming database to correspond to the model's initialisation and were used within the parameterisation. Ancillary information on vegetation and soil parameters (e.g. Leaf Area Index (LAI), Fractional Vegetation Cover (FVC), vegetation height, soil type etc.) was also used directly within the model's initialisation. Such information was acquired in most cases directly from communication with the principal investigators of each respective site, and occasionally from standard literature sources (e.g. Mascart et al., 1991; Carl-

ESDD
6, 217–265, 2015

Appraising the capability of a land biosphere model as a tool in modelling land surface interactions

M. R. North et al.

CC BY

son et al., 1991). The soil type parameters were obtained from the classifications of Clapp and Hornberger (1978) and Cosby et al. (1984), using the soil texture data provided at each CarboEurope test site and information supplied in some instances by the site managers for each experimental site. Similarly, this was also the case for the topographical information that was required in model initialisation. Upon the model initialisation, the latter was executed for each site/day and the 30 min average value of each of the evaluated parameters per site for the period 05:30–23:30 LT was subsequently exported in SPSS for comparisons against the corresponding in-situ data.

3.4 Validation approach

Six statistical metrics were used to evaluate how well the SimSphere predictions matched the observed data for each day on which the model was parameterised and executed. The model's coherence to the observational data was undertaken using the statistical terms suggested by Wilmott (1982). These specifically included the Root Mean Square Difference (RMSD), the linear regression fit model coefficient of determination (R^2), the Bias or Mean Bias Error (MBE), the Scatter or Mean Square Difference (MSD), the Mean Absolute Error (MAE) and the NASH index. The MBE term expresses the accuracy of the model outputs in relation to the in-situ measurements (i.e. low bias = high accuracy) and is used to correct for systematic errors. The MSD term expresses model precision (i.e. low scatter = high precision) and is used to correct for non-systematic errors. The sum of both can be utilised to evaluate overall model accuracy. Table 3 lists the formulae that express the above statistical terms; a detailed description of which can be found for example in Silk (1979), Burt and Barber (1996) and Wilmott (1982). These statistics have also been widely used in similar validation experiments carried out previously (e.g. Wang et al., 2004; Falge et al., 2005; Giertz et al., 2006; Marshall et al., 2013).

In addition, SimSphere's ability to reproduce the diurnal evolution of the examined parameters was evaluated according to the Kramer et al. (2002) criteria described earlier (Sect. 1). All statistical metrics were computed from comparisons performed at

ESDD
6, 217–265, 2015

CC BY

identical 0.5 hourly intervals between the two datasets for each day of comparison. In addition, the same statistical parameters where computed as a summary per experimental CarboEurope site to provide an overview of the model performance per site.

4 Results

4.1 Net Radiation (R_{net}) flux

Table 3 summarises the results of the statistical analysis concerning the comparisons of Net Radiation between the SimSphere estimations and the in-situ measurements. Furthermore, Fig. 3 illustrates the agreement between the in-situ and the predicted R_{net} for all days of comparisons from all experimental sites. Generally, the diurnal variation of the simulated R_{net} was in close correspondence with the observed R_{net} in both shape and magnitude for most of the compared days (although results not shown here for brevity). In overall, SimSphere was able to simulate R_{net} relatively satisfactorily with an average RMSD of 64.65 $W m^{-2}$ and a correlation coefficient of 0.95. A minor underestimation of the in-situ data was also evident for all sites and days combined (MBE = −2.07 $W m^{-2}$). The correspondence between predicted and observed R_{net} fluxes was variable between the individual sites and days included in our study. Indeed, R_{net} showed a significant range of agreement, with RMSD ranging from 24.38 to 98.26 $W m^{-2}$ between the different validation days. Notably, there were increased periods within a number of test sites where simulation accuracy increased depending on the period in which the simulation days were located. For example, for the IT_Ro3 cropland site, error ranges decreased for the period between late April (21 April 2011) and late August (28 August 2011), before increasing in early September (9 September 2011). However, the periods of increased accuracy varied on a per site basis and were only prevalent within the olive plantation (ES_Lju), grassland (IT_Mbo), cropland (IT_Ro3) and deciduous broadleaf forest (IT_Col) sites. Daily R^2 values exhibited less variance with generally more comparable ranges (0.909–0.998) between all the study

ESDD
6, 217–265, 2015

CC BY

days, suggesting a satisfactory agreement between both datasets, also illustrated by the distribution of the points around the 1 : 1 line in Fig. 3. This was also reflected within the NASH index values reported (0.897–0.999).

As can be seen from Table 3, when averaged per site, RMSD showed significantly less variance, exhibiting a range from 55.86 W m^{2} (IT_Lav) to 68.19 W m^{-2} (IT_Col). This trend was also reflected by lower variance in correlation coefficients (R^2 = 0.936–0.970) and NASH index values (0.943–0.981) for the per site averages. The evergreen needle-leaf forest site, IT_Lav, consistently demonstrated the highest model performance in simulating R_{net} with a mean absolute error value of 55.86, 8.79 W m^{-2} lower than the overall average. A weaker agreement was apparent between model predictions of R_{net} and the corresponding observed data in the deciduous broadleaf site, IT_Col (68.19 W m^{-2}), which exhibited the highest RMSD of all sites. MBE between sites showed significant variability, ranging from a moderate underestimation of the in-situ measurements over the evergreen broadleaf forest site (–15.99 W m^{-2}), to a moderate overestimation within the shrubland site (15.02 W m^{-2}). No clear trends in model prediction accuracy dependent on site or land cover type could be identified in our study results.

All in all, SimSphere was able to reproduce the evolution of R_{net} reasonably well in terms of both amplitude and trend which is reflected in the low MSD values of all sites (55.01–68.03 W m^{-2}), particularly so at sites such as IT_Lav (55.01 W m^{-2}) and ES_Agu (60.92 W m^{-2}). Generally, sites which recorded higher scatter results also exhibited higher RMSD results – notably in sites IT_Col (68.03 W m^{-2}) and FR_Pue (66.60 W m^{-2}). Throughout, consistently high NASH values further confirmed the high correspondence between model predictions and observed data.

4.2 Latent heat (LE) flux

Results for the comparison between SimSphere estimated LE flux and the CarboEurope in-situ LE measurements for all days combined exhibited an overall average RMSD error of 62.75 W m^{-2} and a correlation coefficient value of 0.542 respectively

ESDD
6, 217–265, 2015

CC BY

(Table 4). Figure 4 plots the LE flux from the in-situ measurements against the corresponding predicted fluxes from SimSphere for all simulation days from all experimental sites. Although RMSD for the LE parameter showed a better agreement in comparison to the R_{net} parameter (Sect. 4.1), R^2 was significantly lower (a decrease of 0.408). As can be seen from Fig. 4, the distribution of points shows an increased dispersion from the 1 : 1 line in comparison to the R_{net} parameter. There was also an apparent overestimation of the in-situ measurements by the model for this parameter (MBE = 15.78 W m^{-2}). R^2 values varied significantly between all simulation days from 0.020–0.961 (Table 4), suggesting notable discrepancies between the predictions and observations. Additionally, daily RMSD values also varied significantly, reflecting the trends observed in the R^2 statistics. RMSD varied from 22.08 to 86.45 W m^{-2} between all days of simulation. When analysed on a site by site basis, average RMSD exhibited comparable ranges to those reported for the individual simulation days, with RMSD varying from 37.25 W m^{-2} (ES_Agu – Shrubland) to 75.36 W m^{-2} (IT_Col, deciduous broadleaf forest). On a per site basis, in overall, there were noticeable differences in the magnitude of the daily evolution of simulated LE when compared to the in-situ measurements. Specifically, the ES_Agu shrubland site, consistently demonstrated above average alikeness to the in-situ measurements with the lowest RMSD and MAE values of all sites, 37.25 and 25.58 W m^{-2} respectively. Lowest agreement between the LE fluxes predicted from SimSphere and those from the in-situ measurements was in the IT_Col deciduous broadleaf forest site (RMSD = 75.36 W m^{-2}, MAE = 55.86 W m^{-2}) and IT_Mbo grasslands site (RMSD = 74.66 W m^{-2}, MAE = 52.87 W m^{-2}) respectively.

On the whole, SimSphere was consistent in terms of its ability to reproduce in-situ LE fluxes, with low MSD values reported across the majority of sites. However, the IT_Mbo (grassland) and IT_Ro3 (cropland) sites exhibited the largest MSD of 74.58 and 68.48 W m^{-2} respectively, an increase of 15.64 and 9.54 W m^{-2} on the overall average, suggesting a weaker systematic replication of LE fluxes over those sites (Table 4). There was a systematic overestimation of the in-situ measurements by the model simulations for the majority of sites. The only exceptions were for the IT_Mbo and IT_Ro3

ESDD
6, 217–265, 2015

CC BY

sites, exhibiting a small average underestimation (MBE) of −5.11 and −0.87 W m^{-2} respectively. Interestingly, both broad-leaf forest sites, IT_Col (deciduous broad-leaf forest) and FR_Pue (evergreen broad-leaf forest), showed the highest overestimation of LE fluxes with moderately high MBE values of 33.67 and 37.56 W m^{-2} respectively.

4.3 Sensible heat (H) flux

Figure 5 depicts the scatterplot of observed vs. simulated H flux for all experimental sites, whilst Table 5 summarises the relevant statistics concerning the comparisons between the simulated and observed H fluxes for all the days/sites. Results consistently indicated a high ability of the model to accurately simulate H fluxes, with an average RMSD of 55.36 W m^{-2} and an R^2 value of 0.83. A significant improvement in accuracy of this parameter in comparison to both the R_{net} and LE parameters was evident. H flux results exhibited a decrease in overall RMSD of 9.29 and 7.39 W m^{-2} respectively. Similar trends were also evident in both the MBE (−0.08 W m^{-2}) and MSD (55.36 W m^{-2}) results for this parameter, where model performance was better in comparison to both the R_{net} and LE parameters. Although with regards to R^2, the H flux parameter exhibited a minor decrease in correlation (0.83) compared to the R_{net} parameter. When examining the R^2 values for the individual simulation days, there was a significant variation in both correlation coefficients (R^2 = 0.607–0.982) and RMSD (RMSD = 20.03–91.07 W m^{-2}). Notably, there was no clear trend between simulation accuracy and simulation day. Values ranged from 35.50 W m^{-2} (ES_Agu) to 80.41 W m^{-2} (IT_Ro3) on a site by site basis. Similarly to LE flux, the ES_Agu site reported the highest simulation accuracy (RMSD = 35.50 W m^{-2}, R^2 = 0.944, MBE = −7.01 W m^{-2}, MSD = 34.80 W m^{-2}). On the contrary, the cropland site IT_Ro3 consistently reported a less satisfactory agreement between model prediction and in-situ data for H flux. Generally, SimSphere was often unable to represent the peak of H flux across all sites diurnally; this is shown by a scatter of peak values as reported in Fig. 4. However, the model did neither consistently overestimate nor underestimate H flux, but produced a range

ESDD
6, 217–265, 2015

CC BY

of bias values, with an average error of $-0.08\,\mathrm{W\,m^{-2}}$. Both the FR_Pue and ES_Lju sites showed a predominant underestimation of H flux at -25.88 and $-17.17\,\mathrm{W\,m^{-2}}$ respectively. Yet, for the IT_Mbo site, a moderate overestimation of $16.41\,\mathrm{W\,m^{-2}}$ was reported, suggesting land cover type may be related to simulation accuracy, which can be subject of future investigations.

4.4 Air temperature at 1.3 m ($T_{\mathrm{air\ 1.3\,m}}$)

Results obtained confirmed the ability of the model to simulate $T_{\mathrm{air\ 1.3\,m}}$ well, indicating a low average RMSD of 4.1 °C and an average correlation coefficient of 0.631 for all sites and days (Table 6, Fig. 6). Notably, results for R^2 for the specific test days and study sites exhibited significant variance, ranging from 0.237 to 0.939. Such results suggest that time of year and land cover type, and in particular their effect on vegetation, has a noticeable effect on the model's capability to predict $T_{\mathrm{air\ 1.3\,m}}$. RMSD results also exhibited variation between different test days and sites, with values ranging from 1.32 to 7.13 °C.

When simulation accuracy was assessed on a site by site basis, average RMSD ranged from 3.15 °C (IT_Ro3) to 5.12 °C (IT_Col). All sites showed an overestimation of $T_{\mathrm{air\ 1.3\,m}}$, with an average MBE of 3.33 °C. In addition to this, all sites reported low MSD, with an average of just 2.30 °C. This appraises the model's ability to repetitively simulate $T_{\mathrm{air\ 1.3\,m}}$ to a highly acceptable accuracy. The results for the specific sites varied markedly. Simulation over the ES_Agu and IT_Ro3 sites exhibited minor overestimation of the in-situ measurements, with an MBE of 0.72 and 1.01 °C for both sites respectively. Scatter results for both the IT-Lav and It Ro3 sites were very low (and 2.84 and 2.99 °C), appraising the model's ability to produce accurate and stable outputs over these sites. Furthermore, the IT_Ro3 site also produced the highest correlation coefficient ($R^2 = 0.769$) and NASH index (0.769) of all sites. Results for the IT_Col and ES_Lju sites exhibited an increased overestimation of the in-situ measurements (MBE = 3.49 °C) compared to all other sites, with MSD values of 3.74 and 3.95 °C re-

ESDD
6, 217–265, 2015

CC BY

spectively indicating weaker model stability over these sites for all days combined. Results for the ES_Lju site also exhibited lower NASH (–0.054) and R^2 (0.517) values in comparison to all other sites. The latter indicated that the model had some difficulty in reproducing the conditions represented by the in-situ data over the olive orchard experimental site.

4.5 Air temperature at 50 m ($T_{\mathrm{air\ 50\,m}}$)

Figure 7 shows the agreement difference in the simulated $T_{\mathrm{air\ 50\,m}}$ and corresponding in-situ from all experimental sites/days included in this study. The results from the statistical comparisons between the simulated and the measured diurnal $T_{\mathrm{air\ 50\,m}}$ for all the days of the experiment for which observational data were available are summarised in Table 7. As can be observed, the model showed slightly superior performance in predicting $T_{\mathrm{air\ 50\,m}}$ compared to $T_{\mathrm{air\ 1.3\,m}}$, with a decrease of 0.45 °C in overall RMSD to an average value of 3.54 °C. There was a minor overestimation of $T_{\mathrm{air\ 50\,m}}$ by the model (1.40 °C); however, again, an improvement on the results exhibited by the $T_{\mathrm{air\ 1.3\,m}}$ parameter was apparent.

R^2 values per study day for $T_{\mathrm{air\ 50\,m}}$ showed an increased variability in comparison to the $T_{\mathrm{air\ 1.3\,m}}$ parameter, with the overall range in values increasing by 0.173 (0.055 to 0.930). However, daily average RMSD exhibited significantly less variability between sites, ranging from 1.06 °C (IT_Lav) to 6.49 °C (FR_Pue), an improvement of 0.038 °C on the ranges displayed by the $T_{\mathrm{air\ 1.3\,m}}$ results. On a site by site basis, the average range in RMSD in comparison to $T_{\mathrm{air\ 1.3\,m}}$ decreases considerably again, with RMSD ranging from 2.87 °C (IT_Mbo) to 4.25 °C (ES-Lju) for the $T_{\mathrm{air\ 50\,m}}$ parameter. When considering simulation accuracy on a per site basis, it was evident that there were significant differences between the accuracy of the model in simulating both the $T_{\mathrm{air\ 1.3\,m}}$ and the $T_{\mathrm{air\ 50\,m}}$ parameters over the different sites included in our study. Highest simulation accuracy was reported within the It_Mbo (grassland) and IT_Lav (evergreen needle leaf) sites for the $T_{\mathrm{air\ 50\,m}}$ parameter, whereas in comparison, IT_Ro3 (cropland) and ES_Agu (shrubland) were the most accurate sites in terms of $T_{\mathrm{air\ 1.3\,m}}$ prediction by

ESDD
6, 217–265, 2015

cc BY

SimSphere. Both parameters were consistently simulated to high statistical accuracy over the IT_Lav study site. Less satisfactory simulation accuracy was exhibited within the ES_Lju (olive orchards) site for both.

As a whole, the diurnal course of the temperatures predicted by SimSphere was also found to be largely realistically reproduced by the model for most days. A minor overestimation of $T_{\mathrm{air}\ 50\,\mathrm{m}}$ was reported for all validation sites used in this study, with an overall MBE of just 1.35 °C for all days simulated. The extent to which each site overestimated $T_{\mathrm{air}\ 50\,\mathrm{m}}$ was comparable, with a very low range in MBE results from 0.03 °C (ES_Agu) to 2.66 °C (FR_Pue), further appraising the model's ability to produce accurate outputs. Furthermore, such results are a significant improvement on those reported earlier for the $T_{\mathrm{air}\ 1.3\,\mathrm{m}}$ parameter. For all days of simulation, low MSD values were also obtained, with an average MSD of just 3.15 °C. Although there was a slight increase on values reported for the $T_{\mathrm{air}\ 1.3\,\mathrm{m}}$ parameter, results reported still indicate a satisfactory agreement with the in-situ data.

5 Discussion

This study evaluated the ability of the SimSphere land biosphere model to simulate key parameters characterising the Earth's energy and water budget in several European ecosystems. The model was parameterised for a total of 7 CarboEurope sites, representative of a range of ecosystem and environmental conditions. A total of 70 days (10 days per site) from the year 2011 were selected to validate the model's ability to predict Net Radiation (R_{net}), Latent Heat (LE), Sensible Heat (H), and Air temperature (T_{air}) at 1.3 and 50 m. The agreement between the two datasets was evaluated based on a series of computed statistical metrics.

At all sites, R_{net} was systematically well represented by the model, with an average overall RMSD of 64.65 W m^{-2}. In comparison to previous similar validation experiments conducted on earlier SimSphere versions, simulation accuracy of R_{net} reported here is higher, for example more than 20 W m^{-2} in comparison to Ross and

ESDD
6, 217–265, 2015

CC BY

Oke (1988) who validated R_{net} over an urban environment. Respectively, ecosystems which presented high inter-annual change of vegetation phenology, namely olive plantation (ES_Lju), grassland (IT_Mbo), cropland (IT_Ro3) and deciduous broadleaf forest (IT_Col) sites all exhibited distinct periods where model performance was increased. However, these results are significantly better in comparison to those reported by Marshall et al. (2013), who in a similar validation study of the model reported average RMSE of up to 118.46 $W\,m^{-2}$. Akkermans et al. (2014) noted that R_{net} prediction accuracy is also largely dependable on the vegetation and surface characteristics of the respective site and model performance is highly reliant on its representation of the surface vegetation and soil optical properties, most notably surface albedos and emissivities (Falge et al., 2005).

SimSphere showed increased model performance in simulating both LE and H fluxes in comparison to R_{net}; this is confirmed by the low average RMSD and high overall R^2 as reported in Tables 4 and 5. Apart from the general overestimation of LE (MBE = 15.78 $W\,m^{-2}$), results reported show largely acceptable simulation accuracies compared to other analogous studies. Ross and Oke (1988) performed a validation of a previous version of SimSphere over an urban environment of Vancouver, BC. Authors reported acceptable agreement between model output and observed in-situ for H flux (average RMSE = 56 $W\,m^{-2}$) but significant average error distributions for LE fluxes (RMSE = 107 $W\,m^{-2}$). Todhunter and Terjung (1987) further described in detail how earlier versions of the SimSphere model dissipated too much of R_{net} as LE and too little to be lost to H, this correlates well to Ross and Oke's (1988) findings but also the findings reported within; where average bias values indicate general net overestimations of LE flux in the order of 15.78 $W\,m^{-2}$, compared to the slight average underestimation of H at −0.08 $W\,m^{-2}$.

The shrubland site ES_Agu consistently showed remarkably low average RMSD in all parameters assessed, particularly so for LE and H fluxes. This is likely to be a function of the site's location within a water limited environment, where transpiration effects are much lower in amplitude and thus more predictable, especially given the site's rel-

Discussion Paper | Discussion Paper | Discussion Paper | Discussion Paper |
ESDD
6, 217–265, 2015

Appraising the capability of a land biosphere model as a tool in modelling land surface interactions

M. R. North et al.

CC BY

ative homogeneity (Maayar et al., 2001). Marshall et al. (2013) have also suggested that ecosystems which exhibit increased stand complexity and heterogeneity, such as forested environments (particularly those with understory vegetation) can have a profound effect on the overall exchange of mass and energy. The latter cannot be fully represented within the model's parameterisation, therefore accounting for poorer simulation accuracies of LE and H. Additionally, it is widely reported that soil water content is an imperative control to the simulation accuracy of LE and H (Oltchev et al., 2002; Falge et al., 2005). Within our study, soil moisture availability and root zone moisture availability, two of the most sensitive parameters to LE and H flux partitioning (see for example SA study of Petropoulos et al., 2013a, 2014a), were acquired directly from the corresponding daily in-situ measurements. Akkermans et al. (2014) stated that underestimations of LE can largely be attributed to overestimations of H fluxes. Such effects were seen most prominently in our validation site ES_Lju, where a general underestimation of LE (MBE = $-17.17\,\mathrm{W\,m^{-2}}$) partly contributed to the significant overestimation of H flux (MBE = $21.09\,\mathrm{W\,m^{-2}}$).

The model also consistently indicated a satisfactory capability in simulating $T_{\mathrm{air}\ 1.3\,\mathrm{m}}$ and $T_{\mathrm{air}\ 50\,\mathrm{m}}$ in all ecosystems in which it was assessed, with average RMSD similar to values reported in other analogous studies (Ross and Oke, 1988). Poorer simulation accuracies of $T_{\mathrm{air}\ 1.3\,\mathrm{m}}$ were reported in stands where vegetation height exceeds 1.3 m; this is most noticeable in sites ES_Lju, IT_Col and FR_Pue. This suggests that the in-situ data at 1.3 m has a limited representation of the overall transfer of energy and heat seen within the stand; this can explain in part why the model often portrays a general overestimation of $T_{\mathrm{air}\ 1.3\,\mathrm{m}}$ at these particular sites. However, when model predictions are evaluated at 50 m the agreement between modelled and predicted T_{air} is much stronger, with an average RMSD error of 0.6 °C lower than $T_{\mathrm{air}\ 1.3\,\mathrm{m}}$. Ross and Oke (1988) noted that peak values of air temperature should be observed between 10:30–14:30 LST, this is in close correlation to this present study, further appraising SimSphere's representation of T_{air} at both 1.3 and 50 m.

ESDD
6, 217–265, 2015

cc BY

It is also apparent that SimSphere fulfils all 3 of Kramer et al.'s (2002) model assessment criteria, namely accuracy, generality and realism. No significant prediction errors occurred within all of the parameters analysed, further appraising the model's ability to represent numerous environments accurately. Temporal patterns of the predicted parameters were consistent with the patterns found in the corresponding field data, indicating a strong influence of environmental forcing variables (such as global radiation or vapour pressure deficit) on model output. This result is also in agreement to previous SimSphere validation studies (Ross and Oke, 1988). SimSphere has shown high levels of generality, with acceptable simulation accuracies attained in all evaluated sites. In order to improve the model's generality, the inclusion of more northern European sites would act to further test the models applicability within European ecosystems. Realism has been most notable in the simulation of LE and H fluxes, where slight changes in the vegetation phenology or soil surface moisture was accountable for characterising the diurnal evolution of fluxes in all validated sites. On this basis, SimSphere has shown itself to be highly capable of simulating the observed fluxes in both terms of trend and amplitude, with systematically accurate representation of the seasonal effects of vegetation change to flux characteristics.

In the overall evaluation of the results reported, instrumentation uncertainty in the measured parameters themselves should also be partially taken into account when attempting to explain the disagreement between the simulated and observed parameters (Baldocchi et al., 2001; Oncley et al., 2007; Verbeeck et al., 2009). Generally, R_{net} measurement accuracy error is in the order of 10 %, although, an additional 10 % instrumentation uncertainty should be added due to limited view angle/measuring volume (especially in the case of rugged terrains) (Baldocchi et al., 2001). Typical uncertainty in the estimation of the LE and H fluxes using the eddy covariance method generally varies between 10 to 20 % but can be much higher during periods of low flux magnitude and/or limited turbulent mixing such as at night (Petropoulos et al., 2013c). For example, Hollinger and Richardson (2005) showed that uncertainty in flux measurements are inversely proportional to magnitude; the smaller the flux the greater the relative

ESDD
6, 217–265, 2015

CC BY

uncertainty. Also, it should be noted that for some days included in our comparisons, a characteristic of the acquired in-situ data for those days was the presence of many spikes (indicative of very high or very low values). Probable reasons for those spikes could be instrumental errors, horizontal advection of H_2O and CO_2, footprint changes as well as a non-stationarity of turbulent regime within the atmospheric surface layer (Papale et al., 2006; Olchev et al., 2008). For those days, comparisons resulted in a somewhat lower accuracy of model predictions as such conditions cannot be replicated by the model which assumes homogeneity of vegetation canopy and ignores horizontal advection. In terms of SimSphere parameterisation, it is important to note that understory effects of vegetation is a critical influence missing from the model's parameterisation, along with the model's representation of multiple vegetation types. The latter can have a significant effect in more complex vegetation stands (for example the increased presence of understory vegetation in forested environments). This might also be in part responsible for the comparatively poorer overall simulation accuracies exhibited by the model at times.

On the whole, despite the occasionally inferior performance of the model in simulating the examined parameters for some days/sites, SimSphere predictions are significant in terms of the representation of the physical and dynamic processes involved in the interactions of the complex nature of the soil-land–atmosphere system. Moreover, it is important to recognise that uncertainty is inevitable in any model, as a model will never be as complex as the reality it portrays (Denti, 2004). In this way, SimSphere fulfils its objective as a tool to identify expected patterns of change, if not always the magnitudes. The latter indicates its usefulness in practical applications either as a stand-alone tool or in combination with EO data, as done for instance through the implementation of the "triangle" data assimilation technique of Carlson (2007).

ESDD
6, 217–265, 2015

CC BY

6 Concluding remarks

In this paper, key findings from a large scale validation of the SimSphere land biosphere model in numerous European environments are reported. In total, 7 different ecosystems were chosen for validation with 70 simulations made for cloud free days in 2011. A systematic statistical analysis was employed to assess the agreement between model predictions and corresponding in-situ measurements. To our knowledge, this is the first study of its kind, reporting results from an in-depth validation of this models' ability in accurately simulating key parameters characterising land surface processes, particularly so in European ecosystems.

In overall, model performance can largely be described as satisfactory for most of the experimental sites and parameters which were evaluated. Results were also largely comparable to other similar validation attempts of earlier versions of the model performed in dissimilar experimental settings (Todhunter and Terjung, 1987; Ross and Oke, 1988). SimSphere was found to be able to reproduce the diurnal evolution of key parameters at accuracies similar to those reported by others evaluating different SVAT models (Ridler et al., 2012; Marshall et al., 2013; Akkermans et al., 2014). Many factors were identified as having a noteworthy effect on simulation accuracy.

Model comparisons similar to the one conducted in this study can advance our understanding on the amount of complexity required for adequate representation of land surface processes and interactions between different components of our Earth system. An evaluation and analysis of a model performance allows for an increased understanding of the model's representation and helps to identify possible misrepresentations within the observational data. Thus, reported discrepancies found in any validation study such as ours should indeed be regarded as a positive step when evaluating model performance (Denti, 2004; Verbeeck et al., 2009). However, as noted by Denti (2004), any land surface model, by its definition, will never be as complex as the reality it portrays. Nevertheless, in overall, the validation results of this study provide further

ESDD
6, 217–265, 2015

CC BY

independent evidence that SimSphere has a high capability of simulating parameters associated with the Earth's energy balance.

Further efforts should be made to validate SimSphere to numerous global ecosystems to assess its applicability as a universally applied SVAT model. Moreover, as SimSphere's use is being explored synergistically with EO data, perhaps future efforts should be directed towards performing a detailed error budget assessment and evaluating the overriding effects of SimSphere predictions to the overall prediction error of the spatio-temporal estimates of energy fluxes and soil moisture derived from its implementation within the "triangle" technique. These topics and results will be discussed in the next issues.

Acknowledgements. G. P. Petropoulos gratefully acknowledges the financial support provided by the European Commission under the Marie Curie Career Re-Integration Grant "TRANSFORM-EO" project for the completion of this work. Authors would also like to thank Daisy Rendall and Thalia Tataris for their positive contributions to data processing and model implementation. We would also like to thank the PI's of the CarboEurope network for sharing the acquired data of their experimental sites which made this study possible.

References

Akkermans, T., Lauwaet, D., Demuzere, M., Vogel, G., Nouvellon, Y., Ardö, J., and Van Lipzig, N.: Validation and comparison of two soil–vegetation–atmosphere transfer models for tropical Africa, J. Geophys. Res.-Biogeo., 117, G02013, doi:10.1029/2011JG001802, 2012.

Akkermans, T., Thiery, W., and Van Lipzig, N. P.: The regional climate impact of a realistic future, J. Climate, 27, 2714–2734, doi:10.1175/JCLI-D-13-00361.1, 2014.

Amri, R., Zribi, M., Lili-Chabaane, Z., Szczypta, C., Calvet, J. C., and Boulet, G.: FAO-56 Dual Model Combined with Multi-Sensor Remote Sensing for Regional Evapotranspiration Estimations, Remote Sens., 6, 5387–5406, 2014.

Anderson, M. C., Norman, J. M., Kustas, W. P., Houborg, R., Starks, P. J., and Agam, N.: A thermal-based remote sensing technique for routine mapping of land-surface carbon, water and energy fluxes from field to regional scales, Remote Sens. Environ., 112, 4227–4241, 2008.

ESDD

6, 217–265, 2015

Appraising the capability of a land biosphere model as a tool in modelling land surface interactions

M. R. North et al.

Baldocchi, D., Falge, E., Gu, L., Olson, R., Hollinger, D., Running, S., and Wofsy, S.: FLUXNET: a new tool to study the temporal and spatial variability of ecosystem-scale carbon dioxide, water vapour, and energy flux densities, B. Am. Meteorol. Soc., 82, 2415–2434, 2001.

Bellocchi, G., Rivington, M., Donatelli, M., and Matthews, K.: Validation of biophysical models: issues and methodologies. A review, Agron. Sustain. Dev., 30, 109–113, 2010.

Braud, I., Dantas-Antonino, A. C., Vauclin, M., Thony, J. L., and Ruelle, P.: A simple soil–plant–atmosphere transfer model (SiSPAT) development and field verification, J. Hydrol., 166, 213–250, 1995.

Burt, J. E. and Barber, G. M.: Elementary Statistics for Geographers, Longman Ed., London, 504 pp., 1996.

Carlson, T. N.: An overview of the "triangle method" for estimating surface evapotranspiration and soil moisture from satellite imagery, Sensors, 7, 1612–1629, 2007.

Carlson, T. N. and Boland, F. E.: Analysis of urban–rural canopy using a surface heat flux/temperature model, J. Appl. Meteorol., 17, 998–1014, 1978.

Carlson, T. N. and Lynn, B.: The effects of plant water storage on transpiration and radiometric surface temperature, Agr. Forest Meteorol., 57, 171–186, 1991.

Carlson, T. N., Dodd, J. K., Benjamin, S. G., and Cooper, J. N.: Satellite estimation of the surface energy balance, moisture availability and thermal inertia, J. Appl. Meteorol., 20, 6–87, 1981.

Carlson, T. N., Belles, J. E., and Gillies, R. R.: Transient water stress in a vegetation canopy: simulations and measurements, Remote Sens. Environ., 35, 175–186, 1991.

Chauhan, N. S., Miller, S., and Ardanuy, P.: Spaceborne soil moisture estimation at high resolution: a microwave-optical/IR synergistic approach, Int. J. Remote Sens., 22, 4599–4646, 2003.

Clapp, R. B. and Hornberger, G. M.: Empirical equations for some soil hydraulic-properties, Water Resour. Res., 14, 601–604, 1978.

Coudert, B., Ottlé, C., and Briottet, X.: Monitoring land surface processes with thermal infrared data: calibration of SVAT parameters based on the optimisation of diurnal surface temperature cycling features, Remote Sens. Environ., 112, 872–887, 2008.

Culf, A. D., Folken, T., and Gash, J. H. C.: The energy balance closure problem, in: Vegetation, Water, Humans and the Climate, Springer-Verlag, Berlin, 2002.

Deardoff, J. W.: Efficient prediction of ground surface temperature and moisture inclusion of a layer of vegetation, J. Geophys. Res., 83, 1889–1903, 1978.

ESDD

6, 217–265, 2015

CC BY

Denti, G.: Developing a desertification indicator system for a small Mediterranean catchment: a case study from the Serra De Rodes, Alt Emporda, Catalunya, NE Spain, PhD thesis, University of Girona, Girona, 2004.
European Commission: White Paper, Adapting to climate change: towards a European framework for action, COM, Brussels, 1–16, 2009.
European Space Agency, Support to Science Element.: A pathfinder for innovation in Earth Observation, ESA, 2012, available at: http://due.esrin.esa.int/stse/files/document/STSE_report_121016.pdf, last access: 10 July 2013.
Falge, E., Reth, S., Brüggemann, N., Butterbach-Bahl, K., Goldberg, V., Oltchev, A., and Bernhofer, C.: Comparison of surface energy exchange models with eddy flux data in forest and grassland ecosystems of Germany, Ecol. Model., 188, 174–216, 2005.
Feddema, J. J., Oleson, K. W., Bonan, G. B., Mearns, L. O., Buja, L. E., Meehl. G. A., and Washington, W. M.: The importance of land-cover change in simulating future climates, Science, 310, 1674–1678, 2005.
Foken, T., Wimmer, F., Mauder, M., Thomas, C., and Liebethal, C.: Some aspects of the energy balance closure problem, Atmos. Chem. Phys., 6, 4395–4402, doi:10.5194/acp-6-4395-2006, 2006.
Gan, Y., Duan, Q., Gong, W., Tong, C., Sun, Y., Chu, W., Ye, A., Miao, C., and Di, Z.: A comprehensive evaluation of various sensitivity analysis methods: a case study with a hydrological model, Environ. Modell. Softw., 51, 269–285, 2014.
Giertz, S., Diekkrüger, B., and Steup, G.: Physically-based modelling of hydrological processes in a tropical headwater catchment (West Africa) – process representation and multi-criteria validation, Hydrol. Earth Syst. Sci., 10, 829–847, doi:10.5194/hess-10-829-2006, 2006.
Gillies, R. R.: A physically-based land sue classification scheme using remote solar and thermal infrared measurements suitable for describing urbanisation, PhD thesis, University of Newcastle, Newcastle, UK, 121 pp., 1993.
Gillies, R. R., Carlson, T. N., Cui, J., Kustas, W. P., and Humes, K. S.: Verification of the "triangle" method for obtaining surface soil water content and energy fluxes from remote measurements of the Normalized Difference Vegetation Index NDVI and surface radiant temperature, Int. J. Remote Sens., 18, 3145–3166, 1997.
Hollinger, D. and Richardson, A.: Uncertainty in eddy covariance measurements and its application to physiological models, Tree Physiol., 25, 873–885, 2005.

ESDD
6, 217–265, 2015

CC BY

IPCC, Summary report of the IPCC expert meeting on the science of alternative metrics 18–20 March 2009, Oslo, Norway, IPCC-XXX/Doc.13 (31.III.2009), available at: www.ipcc.ch/meetings/session30/doc13.pdf, last access: 8 December 2014.

Kramer, K., Leinonen, I., Bartelink, H. H., Berbigier, P., Borghetti, M., Bernhofer, C., and Vesala, T.: Evaluation of six process-based forest growth models using eddy-covariance measurements of CO_2 and H_2O fluxes at six forest sites in Europe, Global Change Biol., 8, 213–230, 2002.

Li, Z. Q., Yu, G. R., Wen, X. F., Zhang, L. M., Re, C. Y., and Fu, Y. L.: Energy balance closure at ChinaFLUX sites, Sci. China Ser. D., 48, 51–62, 2005.

Liu, Y., Hiyama, T., and Yamaguchi, Y.: Scaling of land surface temperature using satellite data: a case examination on ASTER and MODIS products over a heterogeneous terrain area, Remote Sens. Environ., 105, 115–128, 2006.

Lynn, B. H. and Carlson, T. N.: A stomatal resistance model illustrating plant vs. external control of transpiration, Agr. Forest Meteorol., 52, 5–43, 1990.

Maayar, M., Price, D. T., Delire, C., Foley, J. A., Black, T. A., and Bessemoulin, P.: Validation of the Integrated Biosphere Simulator over Canadian deciduous and coniferous boreal forest stands, J. Geophys. Res.-Atmos., 106, 14339–14355, 2001.

Manabe, S.: Climate and the ocean circulation 1. The atmospheric circulation and the hydrology of the earth's surface, Mon. Weather. Rev., 97, 739–774, 1969.

Marshall, M., Tu, K., Funk, C., Michaelsen, J., Williams, P., Williams, C., Ardö, J., Boucher, M., Cappelaere, B., de Grandcourt, A., Nickless, A., Nouvellon, Y., Scholes, R., and Kutsch, W.: Improving operational land surface model canopy evapotranspiration in Africa using a direct remote sensing approach, Hydrol. Earth Syst. Sci., 17, 1079–1091, doi:10.5194/hess-17-1079-2013, 2013.

Mascart, P., Taconet, O., Pinty, J. P., and Mehrez, M. B.: Canopy resistance formulation and its effect in mesoscale models: a HAPEX perspective, Agr. Forest Meteorol., 54, 319–351, 1991.

Moffat, A., Papale, D., Reichstein, M., Hollinger, D. Y., Richardson, A. D., Barr, A. G., and Beckstein. C.: Comprehensive comparison of gap-filling techniques for eddy covariance net carbon fluxes, Agr. Forest Meteorol., 147, 209–232, 2007.

Monin, A. S. and Obukhov, A.: Basic laws of turbulent mixing in the surface layer of the atmosphere, Contrib. Geophys. Inst. Acad. Sci. USSR, 151, 163–187, 1954.

ESDD
6, 217–265, 2015

Appraising the capability of a land biosphere model as a tool in modelling land surface interactions

M. R. North et al.

cc BY

Olchev, A., Ibrom, A., Ross, T., Falk, U., Rakkibu, G., Radler, K., and Gravenhorst, G.: A modelling approach for simulation of water and carbon dioxide exchange between multi-species tropical rain forest and the atmosphere, Ecol. Model., 212, 122–130, 2008.
Olioso, A., Inoue, Y., Farias, O., Demarty, J., Widneron, J. P., Braud, I., Jacob, F., Lecharpentier, P., Ottle, C., Calvet, J. C., and Brisson, N.: Future directions for advanced evapotranspiration modelling: assimilation of remote sensing data into crop simulation models and SVAT models, Irrig. Drain., 19, 377–412, 2005.
Oliphant, A. J., Grimmond, C. S. B., Zutter, H. N., Schmid, H. P., Su, H.-B., Scott, S. L., Offerle, B., Randolph, J. C., and Ehman, J.: Heat storage and energy balance fluxes for a temperate deciduous forest, Agr. Forest Meteorol., 126, 185–201, 2004.
Oltchev, A., Cermak, J., Nadezhdina, N., Tatarinov, F., Tishenko, A., Ibrom, A., and Gravenhorst, G.: Transpiration of a mixed forest stand: field measurements and simulation using SVAT models, Boreal Environ. Res., 7, 389–397, 2002.
Oncley, S. P., Foken, T., Vogt, R., Kohsiek, W., DeBruin, H. A. R, Berhofer, C., Christen, A., Van Gorsel, E., Grantz, D., Feigenwinter, C., Lehner, I., Liebethal, C., Liu, H., Mauder, M., Pitacco, A., Ribeiro, L., and Weidinger, T.: The Energy Balance Experiment EBEX-2000, Part I: Overview and energy balance, Bound.-Lay. Meteorol., 123, 1–28, 2007.
Papale, D., Reichstein, M., Aubinet, M., Canfora, E., Bernhofer, C., Kutsch, W., Longdoz, B., Rambal, S., Valentini, R., Vesala, T., and Yakir, D.: Towards a standardized processing of Net Ecosystem Exchange measured with eddy covariance technique: algorithms and uncertainty estimation, Biogeosciences, 3, 571–583, doi:10.5194/bg-3-571-2006, 2006.
Petropoulos, G. P. and Carlson, T. N.: Retrievals of turbulent heat fluxes and soil moisture content by remote sensing, in: Advances in Environmental Remote Sensing: Sensors, Algorithms, and Applications, chap. 19, Taylor and Francis, Boca Raton, Florida, 556, 667–502, 2011.
Petropoulos, G. P., Carlson, T., and Wooster, M. J.: An overview of the use of the SimSphere Soil vegetation Atmospheric Transfer (SVAT) model for the study of land atmosphere interactions, Sensors, 9, 4286–4308, 2009a.
Petropoulos, G. P., Wooster, M. J., Kennedy, K., Carlson, T. N., and Scholze, M.: A global sensitivity analysis study of the 1-D SimSphere SVAT model using the GEM SA software, Ecol. Model., 220, 2427–2440, 2009b.
Petropoulos, G. P., Griffiths, H. M., and Tarantola, S.: Towards operational products development from earth observation: exploration of simsphere land surface process model sensitivity

ESDD
6, 217–265, 2015

Appraising the capability of a land biosphere model as a tool in modelling land surface interactions

M. R. North et al.

CC BY

using a GSA approach, in: 7th International Conference on Sensitivity Analysis of 25 Model Output, 1–4 July 2013, Nice, France, 2013a.

Petropoulos, G. P., Griffiths, H., and Tarantola, S.: Sensitivity analysis of the SimSphere SVAT model in the context of EO-based operational products development, Environ. Modell. Softw., 49, 166–179, 2013b.

Petropoulos, G. P., Konstas, I., and Carlson, T. N.: Automation of SimSphere Land Surface Model Use as a Standalone Application and Integration with EO Data for Deriving Key Land Surface Parameters, European Geosciences Union, 7–12 April 2013, Vienna, Austria, 2013c.

Petropoulos, G. P., Griffiths, H. M., Carlson, T. N., Ioannou-Katidis, P., and Holt, T.: SimSphere model sensitivity analysis towards establishing its use for deriving key parameters characterising land surface interactions, Geosci. Model Dev., 7, 1873–1887, doi:10.5194/gmd-7-1873-2014, 2014a.

Petropoulos, G. P., Griffiths, H. M., and Ioannou-Katidis, P.: Sensitivity exploration of SimSphere land surface model towards its use for operational products development from Earth observation data, in: chap. 14, Advancement in Remote Sensing for Environmental Applications, edited by: Mukherjee, S., Gupta, M., Srivastava, P. K., and Islam, T., Springer, Switzerland, 2014b.

Piles, M., Camps, A., Vall-Llossera, M., Corbella, I., Panciera, R., Rudiger, C., Kerr, Y. H., and Walker, J.: Downscaling SMOS-derived soil moisture using MODIS visible/infrared data, IEEE Geosci. Remote S., 49, 3156–3166, 2011.

Prentice, I. C., Liang, X., Medlyn, B. E., and Wang, Y.-P.: Reliable, robust and realistic: the three R's of next-generation land surface modelling, Atmos. Chem. Phys. Discuss., 14, 24811–24861, doi:10.5194/acpd-14-24811-2014, 2014.

Quintana-Seguí, P., Le Moigne, P., Durand, Y., Martin, E., Habets, F., Baillon, M., and Morel, S.: Analysis of near-surface atmospheric variables: validation of the SAFRAN analysis over France, J. Appl. Meteorol. Clim., 47, 92–107, 2008.

Ridler, M. E., Sandholt, I., Butts, M., Lerer, S., Mougin, E., Timouk, F., and Madsen, H.: Calibrating a soil–vegetation–atmosphere transfer model with remote sensing estimates of surface temperature and soil surface moisture in a semi-arid environment, J. Hydrol., 436, 1–12, 2012.

Ross, S. L. and Oke, T. R.: Tests of three urban energy balance models, Bound-Lay. Meteorol., 44, 73–96, 1988.

CC BY

Samaali, M., Courault, D., Bruse, M., Olioso, A., and Occelli, R.: Analysis of a 3-D boundary layer model at local scale: validation on soybean surface radiative measurements, Atmos. Res., 85, 183–198, 2007.
Schrodin, R. and Heise, E.: A new multi-layer version of the DWD Soil Model TERRA_LM, Cosmo Technical Report, No. 2, available at: www.cosmo-model.org (last access: 16 December 2014), 2002.
Sheikh, V., Visser, S., and Stroosnijder, L.: A simple model to predict soil moisture: Bridging Event and Continuous Hydrological (BEACH) modelling, Environ. Modell. Softw., 24, 542–556, 2009.
Silk, J.: Statistical Concepts in Geography, Harper Collins, London, 275 pp., 1979.
Second Space for Hydrology Workshop, European Space Agency (ESA): available at: http://earth.esa.int/hydrospace07/, last access: 16 December 2014.
State of Hydrological Observation Networks, World Meteorological Organization (WMO): available at: http://earth.esa.int/hydrospace07/participants/84231/pres_84231.pdf (last access: 16 December 2014), 2002.
Steinhaeuser, K., Ganguly, A. R., and Chawla, N. V.: Multivariate and multi-scale dependence in the global climate system revealed through complex networks, Clim. Dynam., 39, 889–895, 2012.
Todhunter, P. E. and Terjung, W. H.: Intercomparison of three urban climate models, Bound-Lay. Meteorol., 42, 181–205, 1988.
Tomlin, A. S.: The role of sensitivity and uncertainty analysis in combustion modelling, P. Combust. Inst., 34, 159–176, 2013.
Twine, T. E., Kustas, W. P., Norman, J. M., Cook, D. R., Houser, P. R., Meyers, T. P., Prueger, J. H., Starks, P. J., and Wesely, M. L.: Correcting eddy-covariance flux underestimates over a grassland, Agr. Forest Meteorol., 103, 279–300, 2000.
Vanuytrecht, E., Raes, D., and Willems, P.: Global sensitivity analysis of yield output from the water productivity model, Environ. Modell. Softw., 51, 323–332, 2014.
Verbeeck, H., Samson, R., Granier, A., Montpied, P., and Lemeur, R.: Multi-year model analysis of GPP in a temperate beech forest in France, Ecol. Model., 210, 85–109, 2008.
Wang, Z., Wang, P., and Li, X.: Using MODIS Land Surface Temperature and Normalised Difference Vegetation Index products for monitoring drought in the southern Great Plains, USA, Int. J. Remote. Sens., 25, 61–72, 2004.

ESDD
6, 217–265, 2015

cc BY

Willmott, C. J.: Some comments on the evaluation of model performance, B. Am. Meteorol. Soc., 63, 1309–1313, 1982.
Wilson, K., Goldstein, A., Falge, E., Aubinet, M., Baldocchi, D., Berbigier, P., and Verma, S.: Energy balance closure at FLUXNET sites, Agr. Forest Meteorol., 113, 223–243, 2002.
Wilson, K. B. and Baldocchi, D. D.: Seasonal and inter-annual variability of energy fluxes over a broadleaved temperate deciduous forest in North America, Agr. Forest Meteorol., 100, 1–18, 2000.

ESDD
6, 217–265, 2015

CC BY

Table 1. Summary of the main SimSphere inputs. The units of each of the model inputs are also provided in parentheses where applicable.

Name of the model input	Process in which parameter is involved	Min value	Max value
Slope (degrees)	TIME and LOCATION	0	45
Aspect (degrees)	TIME and LOCATION	0	360
Station Height (meters)	TIME and LOCATION	0	4.92
Fractional Vegetation Cover (%)	VEGETATION	0	100
LAI ($m^2 m^{-2}$)	VEGETATION	0	10
Foliage emissivity (unitless)	VEGETATION	0.951	0.990
[Ca] (external [CO_2] in the leaf) (ppmv)	VEGETATION	250	710
[Ci] (internal [CO_2] in the leaf) (ppmv)	VEGETATION	110	400
[03] (ozone concentration in the air) (ppmv)	VEGETATION	0.0	0.25
Vegetation height (meters)	VEGETATION	0.021	20.0
Leaf width (meters)	VEGETATION	0.012	1.0
Minimum Stomatal Resistance ($s m^{-1}$)	PLANT	10	500
Cuticle Resistance ($s m^{-1}$)	PLANT	200	2000
Critical leaf water potential (bar)	PLANT	−30	−5
Critical solar parameter ($W m^{-2}$)	PLANT	25	300
Stem resistance ($s m^{-1}$)	PLANT	0.011	0.150
Surface Moisture Availability (vol/vol)	HYDROLOGICAL	0	1
Root Zone Moisture Availability (vol/vol)	HYDROLOGICAL	0	1
Substrate Max. Volum. Water Content (vol/vol)	HYDROLOGICAL	0.01	1
Substrate climatol. mean temperature (°C)	SURFACE	20	30
Thermal inertia ($W m^{-2} K^{-1}$)	SURFACE	3.5	30
Ground emissivity (unitless)	SURFACE	0.951	0.980
Atmospheric Precipitable water (cm)	METEOROLOGICAL	0.05	5
Surface roughness (meters)	METEOROLOGICAL	0.02	2.0
Obstacle height (meters)	METEOROLOGICAL	0.02	2.0
Fractional Cloud Cover (%)	METEOROLOGICAL	1	10
RKS (satur. thermal conduct., Cosby et al., 1984)	SOIL	0	10
Cosby B (see Cosby et al., 1984)	SOIL	2.0	12.0
THM (satur.vol. water cont.) (Cosby et al., 1984)	SOIL	0.3	0.5
PSI (satur. water potential) (Cosby et al., 1984)	SOIL	1	7
Wind direction (degrees)	WIND SOUNDING PROFILE	0	360
Wind speed (knots)	WIND SOUNDING PROFILE	–	–
Altitude (1000's feet)	WIND SOUNDING PROFILE	–	–
Pressure (mBar)	MOISTURE SOUNDING PROFILE	–	–
Temperature (Celsius)	MOISTURE SOUNDING PROFILE	–	–
Temperature-Dewpoint Temperature (Celsius)	MOISTURE SOUNDING PROFILE	–	–

ESDD
6, 217–265, 2015

CC BY

Table 2. Some of the main characteristics of the selected CarboEurope sites used for SimSphere validation.

Site Name	Site Abbreviation	County	Geographic Location	PFT	Ecosystem Type	Dominant Species	Elevation	Climate
Llano de los Juanes	ES_Lju	SPAIN	36.9266/−2.1521	OLI	Olive Plantation	*Oleaeuropea*, Macchia	1622 m	Warm Temperate with dry, hot summer
Collelongo-SelvaPiana	IT_Col	ITALY	41.8493/13.5881	DBF	Deciduous Broadleaf Forest	*Fagus sylvatica*	1645 m	Warm temperate fully humid with warm summer
Monte Modone	IT_Mbo	ITALY	46.0296/11.0829	GRA	Grassland	Alpine meadow	1547 m	Snow fully humid warm summer
Aguamarga	ES_Agu	SPAIN	36.8347/−2.2511	SHR	Annual Broadleaf Shrub	Sumac (*Rhus*), Toyon (*Heteromeles*) and Coffeeberry (*Rhamnus*) Species	195 m	Arid Steppe Cold
Lavarone	IT_Lav	ITALY	45.9553/11.2812	ENL	Evergreen Needle Leaf forest	*Pinus sylvestris*	1353 m	Warm temperate fully humid with warm summer
Puechabon	FR_Pue	FRANCE	43.7414/3.5958	EBF	Evergreen Broadleaf forest	*Quercus ilex*	211 m	Warm Temperate with dry, hot summer
Roccarepampani	IT_Ro3	ITALY	42.3753/11.9154	CRO	Cropland	Cereal Crop	320 m	Warm Temperate with dry, hot summer

ESDD
6, 217–265, 2015

ESDD
6, 217–265, 2015

Table 3. An overview of the statistical measures implemented in this study to evaluate SimSphere's outputs against the corresponding in-situ data.

Name	Description	Mathematical Definition
Bias/MBE	Bias (accuracy) or Mean Bias Error	$\text{bias} = \frac{1}{N}\sum_{i=1}^{N}(P_i - O_i)$
R^2	Linear Correlation Coefficient of Determination of P_i to O_i	$R^2 = \left[\sum_{i=1}^{N}\left(P_i - \overline{P}\right)\left(O_i - \overline{O}\right) \Big/ \left[\sum_{i=1}^{N}\left(O_i - \overline{O}\right)^2 \sum_{i=1}^{N}\left(P_i - \overline{O}\right)^2\right]^{0.5}\right]^2$
Scatter/MSD	Scatter (precision) or Mean Square Difference	$\text{scatter} = \frac{1}{(N-1)}\sum_{i=1}^{N}\left(P_i - O_i - \overline{(P_i - O_i)}\right)^2$
RMSD	Root Mean Square Difference	$\text{RMSD} = \sqrt{\text{bias}^2 + \text{scatter}^2}$
MAE	Mean Absolute Error	$\text{MAD} = N^{-1}\sum_{i=1}^{N}\lvert P_i - O_i\rvert$
NASH	Nash Sutcliffe Efficiency	$\text{NASH} = 1 - \left[\frac{\sum_{i=1}^{N}(O_i - S_i)^2}{\sum_{i=1}^{N}\left(O_i - \overline{O}\right)^2}\right]$

Table 4. An overview of R_{net} simulation accuracy.

Site	PFT	Day	Statistical Test					Site	PFT	Day	Statistical Test				
			Bias	Scatter	RMSD	MAE	NASH				Bias	Scatter	RMSD	MAE	NASH
ES_Lju	OLI	14 Apr 2011	−24.55	42.31	48.91	32.45	0.921	IT_Ro3	CRO	9 Apr 2011	−8.20	85.76	86.16	76.40	0.912
		9 May 2011	−19.34	60.31	63.33	47.55	0.976			11 Apr 2011	−52.87	46.21	70.22	55.97	0.913
		24 Jun 2011	12.18	67.54	68.63	57.97	0.916			18 Apr 2011	13.74	80.88	82.03	72.17	0.990
		27 Jun 2011	6.06	66.98	67.25	47.26	0.978			21 Apr 2011	24.95	56.34	61.62	55.09	0.982
		19 Jul 2011	26.05	57.38	63.01	44.21	0.934			20 Jun 2011	−12.51	53.15	54.60	48.95	0.937
		28 Jul 2011	34.52	56.12	65.89	47.60	0.971			26 Jun 2011	−22.36	48.39	53.30	42.70	0.972
		4 Aug 2011	15.06	51.08	53.25	33.81	0.930			24 Aug 2011	13.94	54.53	56.28	41.84	0.961
		22 Aug 2011	8.26	57.55	58.14	47.33	0.899			28 Aug 2011	−8.98	59.95	60.62	51.20	0.899
		25 Aug 2011	10.23	59.03	59.91	49.44	0.978			9 Sep 2011	−19.92	67.62	70.49	62.77	0.897
		28 Sep 2011	−19.69	92.19	94.27	78.84	0.998			11 Sep 2011	2.40	68.15	68.19	55.23	0.971
		Average	4.88	64.78	64.96	48.65	0.950			Average	−6.98	66.53	66.90	56.23	0.943
IT_Col	DBF	26 Jun 2011	−29.91	67.82	74.12	52.94	0.969	IT_Lav	EN L	27 Jun 2011	−24.60	57.52	62.56	46.13	0.971
		8 Jul 2011	−23.15	46.34	51.80	41.84	0.978			3 Jul 2011	−60.69	39.12	72.21	63.35	0.986
		13 Jul 2011	−12.95	56.81	58.27	50.16	0.934			9 Jul 2011	−35.90	57.43	67.73	58.59	0.971
		18 Jul 2011	−23.69	54.99	59.87	48.72	0.978			11 Aug 2011	−16.51	31.22	35.32	30.06	0.998
		11 Aug 2011	−10.67	63.23	64.12	50.03	0.974			12 Aug 2011	−0.79	31.24	31.25	24.10	0.996
		23 Aug 2011	14.50	64.17	65.79	54.93	0.940			20 Aug 2011	3.59	31.32	31.53	21.85	0.975
		11 Sep 2011	40.85	53.96	67.67	47.63	0.899			21 Aug 2011	23.69	29.01	37.46	32.13	0.989
		15 Sep 2011	38.95	59.52	71.13	52.79	0.969			24 Aug 2011	47.45	25.99	54.10	47.45	0.990
		16 Sep 2011	18.84	70.23	72.71	50.39	0.999			9 Sep 2011	33.71	46.83	57.70	49.08	0.979
		17 Sep 2011	44.54	54.46	70.36	47.23	0.920			30 Sep 2011	58.84	78.66	98.26	78.02	0.954
		Average	4.61	68.03	68.19	51.16	0.956			Average	−9.70	55.01	55.86	44.02	0.981
IT_Mbo	GRA	10 Apr 2011	−45.49	54.34	70.87	47.71	0.979	FR_Pue	EBF	6 Apr 2011	−48.91	48.89	69.15	52.63	0.978
		10 May 2011	−22.05	41.00	46.56	37.14	0.936			9 Apr 2011	−39.03	51.27	64.43	50.03	0.913
		25 Jun 2011	−11.70	21.39	24.38	18.92	0.901			16 Apr 2011	−57.09	45.67	73.11	57.57	0.932
		3 Jul 2011	−12.38	66.20	67.35	56.63	0.978			17 May 2011	−27.98	49.22	56.62	46.95	0.946
		24 Aug 2011	40.61	55.84	69.04	46.81	0.925			28 May 2011	−38.36	48.14	61.55	50.92	0.961
		25 Aug 2011	41.22	61.04	73.66	50.97	0.978			19 Jun 2011	−58.10	49.41	76.27	64.97	0.947
		13 Sep 2011	−23.86	80.95	84.39	78.38	0.963			8 Jul 2011	−27.62	38.41	47.31	37.66	0.975
		21 Sep 2011	−21.12	75.19	78.10	69.16	0.910			26 Sep 2011	49.90	44.96	67.17	49.90	0.963
		26 Sep 2011	−3.44	67.29	67.38	59.95	0.912			14 Sep 2011	60.09	48.58	77.27	60.09	0.978
		30 Sep 2011	−5.05	49.55	49.81	43.63	0.978			20 Sep 2011	47.71	62.85	78.91	51.51	0.938
		Average	−6.33	65.07	65.38	50.93	0.946			Average	−15.99	66.60	68.49	52.47	0.953
ES_Agu	SHR	07 Apr 2011	−49.42	23.11	54.55	49.42	0.978								
		27 Apr 2011	−62.87	26.14	68.09	62.87	0.963								
		8 May 2011	−41.11	19.67	45.58	41.11	0.974								
		14 May 2011	−14.87	34.17	37.26	33.38	0.954								
		23 May 2011	−24.01	24.79	34.51	31.38	0.960								
		13 Jul 2011	27.95	26.78	38.71	32.17	0.980								
		29 Jul 2011	52.86	64.52	83.40	68.43	0.979								
		14 Aug 2011	55.68	50.21	74.97	67.51	0.968								
		26 Aug 2011	59.11	52.30	78.92	70.46	0.989								
		7 Sep 2011	41.81	48.79	64.25	59.21	0.972								
		Average	15.02	60.92	62.75	53.40	0.972								
ALL SITES		AVERAGE	−2.07	63.85	64.65	50.98	0.96								

Table 5. An overview of LE simulation accurancy.

Site	PFT	Day	Statistical Test					Site	PFT	Day	Statistical Test				
			Bias	Scatter	RMSD	MAE	NASH				Bias	Scatter	RMSD	MAE	NASH
ES_Lju	OLI	14 Apr 2011	13.10	43.69	45.62	34.00	0.987	IT_Ro3	CRO	9 Apr 2011	−34.88	54.19	64.45	39.69	0.996
		9 May 2011	−8.48	37.57	38.51	26.45	0.993			11 Apr 2011	−39.35	43.02	58.30	41.49	0.997
		24 Jun 2011	42.62	62.22	75.42	63.34	0.977			18 Apr 2011	−17.47	21.90	28.02	20.97	0.998
		27 Jun 2011	46.98	59.15	75.53	60.96	0.968			21 Apr 2011	1.65	27.69	27.74	20.70	0.998
		19 Jul 2011	17.78	25.03	30.70	23.02	0.954			20 Jun 2011	51.85	54.15	74.97	55.86	0.954
		28 Jul 2011	26.35	23.88	35.57	30.00	0.961			26 Jun 2011	38.33	31.82	49.81	39.17	0.960
		4 Aug 2011	−13.97	24.09	27.85	21.57	0.966			24 Aug 2011	12.15	28.29	30.79	22.73	0.984
		22 Aug 2011	−3.40	38.77	38.92	28.53	0.987			28 Aug 2011	18.05	26.51	32.07	23.96	0.973
		25 Aug 2011	22.97	33.43	40.56	29.31	0.902			9 Sep 2011	46.93	45.17	65.14	47.73	0.972
		28 Sep 2011	22.00	28.76	36.21	26.91	0.903			11 Sep 2011	49.09	54.13	73.07	51.67	0.986
		Average	21.09	51.49	55.64	37.22	0.983			Average	−0.87	68.48	68.48	47.51	0.982
IT_Col	DBF	26 Jun 2011	26.53	30.72	40.59	30.21	0.915	IT_Lav	EN L	27 Jun 2011	−9.09	38.54	39.59	29.72	0.938
		8 Jul 2011	2.34	71.20	71.24	51.70	0.936			3 Jul 2011	23.40	41.88	47.97	38.47	0.973
		13 Jul 2011	33.33	53.23	62.81	47.75	0.976			9 Jul 2011	−16.39	55.28	57.66	41.60	0.912
		18 Jul 2011	35.85	70.07	78.71	62.73	0.935			11 Aug 2011	32.47	44.84	55.36	41.66	0.899
		11 Aug 2011	32.46	68.31	75.63	65.57	0.894			12 Aug 2011	29.70	67.43	73.68	59.10	0.937
		23 Aug 2011	−25.34	81.15	85.01	50.98	0.900			20 Aug 2011	31.48	80.52	86.45	63.16	0.936
		11 Sep 2011	56.10	42.26	70.23	56.10	0.986			21 Aug 2011	−12.13	45.44	47.04	33.46	0.938
		15 Sep 2011	60.69	49.42	78.27	61.47	0.984			24 Aug 2011	−21.87	57.06	61.11	46.97	0.989
		16 Sep 2011	50.25	47.72	69.30	53.45	0.987			9 Sep 2011	27.18	69.22	74.37	59.71	0.935
		17 Sep 2011	6.74	26.51	27.35	21.59	0.993			30 Sep 2011	9.78	40.27	55.69	48.69	0.913
		Average	33.67	67.43	75.36	55.86	0.951			Average	8.47	58.32	58.93	41.39	0.937
IT_Mbo	GRA	10 Apr 2011	16.85	25.39	30.47	21.85	0.989	FR_Pue	EBF	6 Apr 2011	52.85	57.24	77.91	56.05	0.980
		10 May 2011	−35.35	42.72	55.45	40.52	0.913			9 Apr 2011	−17.44	39.39	43.08	25.79	0.996
		25 Jun 2011	6.87	59.93	60.33	49.33	0.976			16 Apr 2011	43.76	41.67	60.43	45.93	0.977
		3 Jul 2011	−26.51	73.75	78.37	56.20	0.911			17 May 2011	45.00	59.73	74.78	56.06	0.990
		24 Aug 2011	−19.29	51.79	55.27	37.79	0.978			28 May 2011	46.25	61.55	76.99	55.46	0.985
		25 Aug 2011	26.85	68.15	73.25	61.21	0.936			19 Jun 2011	28.64	43.41	52.01	39.13	0.993
		13 Sep 2011	−8.09	44.20	44.93	36.71	0.998			8 Jul 2011	22.05	38.52	44.38	33.47	0.983
		21 Sep 2011	14.93	53.34	55.39	34.19	0.936			26 Sep 2011	49.04	44.60	66.28	50.75	0.985
		26 Sep 2011	14.52	52.12	54.10	39.33	0.978			14 Sep 2011	62.28	39.97	74.00	62.28	0.954
		30 Sep 2011	26.21	37.65	45.88	33.52	0.980			20 Sep 2011	11.54	19.56	22.71	18.02	0.987
		Average	−3.45	74.58	74.66	52.87	0.959			Average	37.56	57.77	68.91	47.46	0.988
ES_Agu	SHR	7 Apr 2011	−20.76	30.09	36.55	25.02	0.990								
		27 Apr 2011	−21.86	29.03	36.34	28.04	0.994								
		8 May 2011	−9.68	21.12	23.23	16.54	0.996								
		14 May 2011	9.05	20.14	22.08	17.51	0.990								
		23 May 2011	10.84	25.10	27.35	19.64	0.986								
		13 Jul 2011	27.01	28.63	39.36	31.06	0.884								
		29 Jul 2011	34.47	25.94	43.14	34.81	0.754								
		14 Aug 2011	25.42	24.42	35.25	28.31	0.947								
		26 Aug 2011	28.00	52.61	59.60	40.41	0.975								
		7 Sep 2011	36.65	37.96	52.76	39.47	0.953								
		Average	13.99	34.53	37.25	25.58	0.947								
ALL SITES		AVERAGE	15.78	58.94	62.75	43.98	0.964								

ESDD
6, 217–265, 2015

CC BY

Table 6. An overview of H simulation accurancy.

Site	PFT	Day	Statistical Test					Site	PFT	Day	Statistical Test				
			Bias	Scatter	RMSD	MAE	NASH				Bias	Scatter	RMSD	MAE	NASH
ES_Lju	OLI	14 Apr 2011	−29.24	44.75	53.45	39.51	0.985	IT_Ro3	CRO	9 Apr 2011	10.92	39.80	41.27	26.92	0.934
		9 May 2011	−11.76	32.57	34.63	30.29	0.963			11 Apr 2011	31.67	30.24	43.79	34.75	0.919
		24 Jun 2011	−47.07	39.11	61.20	48.54	0.945			18 Apr 2011	42.10	42.34	59.71	44.00	0.958
		27 Jun 2011	−28.81	38.98	48.47	37.58	0.948			21 Apr 2011	33.35	52.28	62.01	42.53	0.961
		19 Jul 2011	−27.46	38.74	47.48	35.77	0.978			20 Jun 2011	−9.57	73.29	73.91	52.42	0.958
		28 Jul 2011	−43.87	50.48	66.88	51.27	0.915			26 Jun 2011	17.25	89.42	91.07	70.44	0.983
		4 Aug 2011	18.95	38.42	42.84	31.95	0.934			24 Aug 2011	16.30	43.62	46.56	36.97	0.917
		22 Aug 2011	−3.39	51.14	51.25	39.75	0.964			28 Aug 2011	−17.29	48.32	51.32	30.11	0.913
		25 Aug 2011	17.21	52.08	54.85	44.13	0.964			9 Sep 2011	−15.89	39.23	42.32	28.03	0.978
		28 Sep 2011	13.23	41.60	43.65	29.29	0.978			11 Sep 2011	−22.61	61.45	65.48	44.20	0.928
		Average	−17.17	60.22	62.62	43.97	0.957			Average	15.53	70.23	71.93	47.95	0.945
IT_Col	DBF	26 Jun 2011	1.74	46.77	46.80	33.26	0.899	IT_Lav	EN L	27 Jun 2011	−22.70	68.75	72.40	51.93	0.968
		8 Jul 2011	18.13	64.78	67.27	51.57	0.924			3 Jul 2011	−35.97	64.90	74.20	54.32	0.974
		13 Jul 2011	9.77	44.49	45.55	41.51	0.970			9 Jul 2011	−25.35	48.49	54.72	40.30	0.913
		18 Jul 2011	12.29	57.20	58.50	51.31	0.941			11 Aug 2011	5.65	41.04	41.42	32.01	0.978
		11 Aug 2011	−3.40	37.51	37.66	29.44	0.991			12 Aug 2011	0.32	32.85	32.85	25.04	0.963
		23 Aug 2011	55.49	53.01	76.74	60.69	0.997			20 Aug 2011	7.77	56.67	57.20	38.05	0.918
		11 Sep 2011	32.16	37.20	49.17	36.64	0.969			21 Aug 2011	9.11	51.09	51.90	38.97	0.978
		15 Sep 2011	21.18	73.90	76.88	62.74	0.879			24 Aug 2011	18.93	56.46	59.55	46.52	0.899
		16 Sep 2011	23.20	43.50	49.30	41.64	0.969			9 Sep 2011	3.34	71.63	71.71	55.63	0.910
		17 Sep 2011	−0.51	59.69	59.69	45.19	0.914			30 Sep 2011	41.43	41.04	58.31	43.60	0.989
		Average	14.72	58.78	60.59	46.84	0.945			Average	−6.72	56.95	57.34	39.18	0.949
IT_Mbo	GRA	10 Apr 2011	−29.74	51.93	59.84	48.15	0.910	FR_Pue	EBF	6 Apr 2011	−36.45	36.93	51.89	38.72	0.978
		10 May 2011	0.29	20.03	20.03	16.50	0.971			9 Apr 2011	−4.73	61.85	62.03	46.98	0.995
		25 Jun 2011	4.97	32.86	33.23	25.14	0.896			16 Apr 2011	−42.22	50.00	65.44	49.12	0.914
		3 Jul 2011	15.82	67.80	69.62	42.00	0.941			17 May 2011	−50.66	49.10	70.55	53.69	0.968
		24 Aug 2011	36.06	22.46	42.48	37.55	0.879			28 May 2011	−4.18	60.90	61.04	49.30	0.978
		25 Aug 2011	32.11	22.49	39.20	32.69	0.986			19 Jun 2011	−37.85	59.70	70.69	64.09	0.925
		13 Sep 2011	15.15	26.73	30.73	22.44	0.976			8 Jul 2011	−14.58	40.37	42.93	35.78	0.946
		21 Sep 2011	31.57	24.50	39.96	32.22	0.936			26 Sep 2011	11.57	31.31	33.38	26.11	0.917
		26 Sep 2011	16.48	13.24	21.14	17.15	0.914			14 Sep 2011	23.07	42.11	48.01	38.77	0.913
		30 Sep 2011	41.43	41.04	58.31	43.60	0.989			20 Sep 2011	−6.86	28.55	29.36	20.38	0.979
		Average	16.41	40.97	44.13	31.74	0.940			Average	−16.29	52.98	55.43	42.29	0.951
ES_Agu	SHR	7 Apr 2011	−1.09	30.30	30.32	25.05	0.991								
		27 Apr 2011	−17.07	24.53	29.89	24.17	0.930								
		8 May 2011	−8.29	29.72	30.85	22.23	0.978								
		14 May 2011	−10.76	24.77	27.00	22.46	0.915								
		23 May 2011	−30.75	33.29	45.32	33.51	0.997								
		13 Jul 2011	−27.78	33.14	43.24	31.19	0.937								
		29 Jul 2011	−4.41	37.58	37.84	28.45	0.914								
		14 Aug 2011	20.68	35.58	41.16	31.22	0.989								
		26 Aug 2011	8.19	47.52	48.22	34.04	0.937								
		7 Sep 2011	0.07	30.02	30.02	22.99	0.993								
		Average	−7.01	34.80	35.50	25.03	0.958								
ALL SITES		AVERAGE	−0.08	53.56	55.36	39.57	0.95								

ESDD
6, 217–265, 2015
Appraising the capability of a land biosphere model as a tool in modelling land surface interactions
M. R. North et al.

CC BY

ESDD
6, 217–265, 2015

Title Page
Abstract | Introduction
Conclusions | References
Tables | Figures
◀I | ▶I
◀ | ▶
Back | Close
Full Screen / Esc
Printer-friendly Version
Interactive Discussion

CC BY

Table 7. An overview of $T_{\mathrm{air\ 1.3\,m}}$ simulation accurancy.

Site	PFT	Day	Statistical Test					Site	PFT	Day	Statistical Test				
			Bias	Scatter	RMSD	MAE	NASH				Bias	Scatter	RMSD	MAE	NASH
ES_Lju	OLI	14 Apr 2011	0.75	2.93	3.03	2.56	0.330	IT_Ro3	CRO	9 Apr 2011	2.19	2.81	3.56	3.13	0.887
		9 May 2011	3.87	2.58	4.65	3.87	0.631			11 Apr 2011	0.05	3.24	3.24	2.85	0.944
		24 Jun 2011	−2.04	1.92	2.80	2.13	−0.448			18 Apr 2011	2.24	2.91	3.67	2.82	0.909
		27 Jun 2011	1.99	3.92	4.40	3.86	−1.460			21 Apr 2011	1.04	2.74	2.93	2.39	0.938
		19 Jul 2011	2.64	3.14	4.11	3.35	0.612			20 Jun 2011	0.49	4.89	4.91	4.06	0.903
		28 Jul 2011	5.45	2.59	6.03	5.45	0.215			26 Jun 2011	3.70	3.44	5.06	3.82	0.853
		4 Aug 2011	3.61	3.55	5.06	4.53	−0.971			24 Aug 2011	n/a	n/a	n/a	n/a	n/a
		22 Aug 2011	3.35	2.76	4.34	3.61	0.695			28 Aug 2011	n/a	n/a	n/a	n/a	n/a
		25 Aug 2011	5.31	3.94	6.61	5.68	0.049			9 Sep 2011	n/a	n/a	n/a	n/a	n/a
		28 Sep 2011	3.59	4.95	6.12	5.49	−0.198			11 Sep 2011	n/a	n/a	n/a	n/a	n/a
		Average	2.75	3.95	4.82	4.02	−0.054			Average	1.01	2.99	3.15	1.97	0.905
IT_Col	DBF	26 Jun 2011	5.29	2.33	5.78	5.31	0.493	IT_Lav	EN L	27 Jun 2011	2.19	1.80	2.83	2.44	0.359
		8 Jul 2011	1.21	67.09	7.13	2.42	0.757			3 Jul 2011	0.54	1.20	1.32	1.14	0.855
		13 Jul 2011	6.01	1.74	6.26	6.01	0.396			9 Jul 2011	2.78	3.09	4.16	3.64	−0.607
		18 Jul 2011	2.83	2.08	3.51	3.12	0.766			11 Aug 2011	2.81	2.84	3.99	4.00	−0.019
		11 Aug 2011	3.98	2.92	4.94	4.02	0.806			12 Aug 2011	0.02	2.06	2.06	1.79	0.594
		23 Aug 2011	−1.35	2.05	2.46	2.06	0.904			20 Aug 2011	0.64	2.53	2.61	2.18	0.469
		11 Sep 2011	5.35	1.71	5.62	5.35	0.740			21 Aug 2011	1.54	2.46	2.90	2.59	0.353
		15 Sep 2011	1.25	1.67	2.09	1.61	0.929			24 Aug 2011	1.78	2.76	3.28	2.67	0.236
		16 Sep 2011	0.24	1.74	1.75	1.40	0.944			9 Sep 2011	4.47	3.96	5.97	5.30	−0.070
		17 Sep 2011	1.58	2.12	2.65	2.16	0.915			30 Sep 2011	2.70	2.01	3.21	2.97	0.871
		Average	3.49	3.74	5.12	4.08	0.765			Average	1.68	2.84	3.30	2.51	0.304
IT_Mbo	GRA	10 Apr 2011	3.31	0.99	3.46	3.31	0.177	FR_Pue	EBF	6 Apr 2011	5.83	1.69	6.07	5.83	0.662
		10 May 2011	1.40	2.47	2.84	1.98	0.669			9 Apr 2011	2.26	3.58	4.23	3.94	0.794
		25 Jun 2011	1.03	0.91	1.38	1.26	0.845			16 Apr 2011	2.36	1.10	2.60	2.36	0.832
		3 Jul 2011	4.81	1.44	5.02	4.81	0.320			17 May 2011	1.68	1.05	1.98	1.78	0.866
		24 Aug 2011	2.55	1.21	2.82	2.55	0.600			28 May 2011	5.21	1.93	5.56	5.21	0.554
		25 Aug 2011	2.18	3.62	4.22	3.80	0.425			19 Jun 2011	3.49	1.05	3.65	3.49	0.355
		13 Sep 2011	4.21	0.96	4.32	4.21	0.465			8 Jul 2011	2.79	0.89	2.93	2.79	0.766
		21 Sep 2011	0.98	1.58	1.86	1.27	0.883			14 Sep 2011	3.33	2.46	4.14	3.33	0.747
		26 Sep 2011	2.31	1.84	2.95	2.35	0.739			20 Sep 2011	−1.67	2.46	2.97	2.69	0.796
		30 Sep 2011	2.01	1.18	2.33	2.03	0.764			26 Sep 2011	1.96	2.25	2.99	2.15	0.883
		Average	3.34	3.18	4.61	3.46	0.589			Average	3.13	3.07	4.38	3.76	0.725
ES_Agu	SHR	7 Apr 2011	1.33	3.80	4.02	3.62	0.610								
		27 Apr 2011	0.02	2.59	2.59	2.13	0.803								
		8 May 2011	−0.75	2.35	2.47	2.10	0.821								
		14 May 2011	1.17	2.28	2.56	2.09	0.844								
		23 May 2011	−0.21	1.85	1.86	1.48	0.870								
		13 Jul 2011	1.94	4.21	4.63	3.76	0.722								
		29 Jul 2011	1.46	3.46	3.75	3.19	0.583								
		14 Aug 2011	0.38	3.75	3.77	3.17	0.871								
		26 Aug 2011	1.94	4.21	4.63	3.76	0.722								
		7 Sep 2011	3.07	2.79	4.15	3.49	0.493								
		Average	0.72	3.52	3.59	2.72	0.734								
All Sites		Average	2.30	3.33	4.14	3.22	0.567								

Table 8. An overview of $T_{\text{air 50 m}}$ simulation accurancy.

Site	PFT	Day	Statistical Test					Site	PFT	Day	Statistical Test				
			Bias	Scatter	RMSD	MAE	NASH				Bias	Scatter	RMSD	MAE	NASH
ES_Lju	OLI	14 Apr 2011	0.84	1.56	1.77	1.56	0.591	IT_Ro3	CRO	9 Apr 2011	1.56	3.48	3.81	3.49	0.874
		9 May 2011	0.72	3.77	3.84	3.35	0.457			11 Apr 2011	0.05	4.73	4.73	4.28	0.916
		24 Jun 2011	1.01	3.40	3.55	2.80	0.893			18 Apr 2011	2.55	4.35	5.04	3.98	0.871
		27 Jun 2011	1.14	4.69	4.82	4.40	−1.804			21 Apr 2011	0.69	4.36	4.41	3.90	0.899
		19 Jul 2011	0.30	4.70	4.71	4.04	0.846			20 Jun 2011	0.49	4.89	4.91	4.06	0.903
		28 Jul 2011	3.31	2.62	4.22	3.46	0.501			26 Jun 2011	−2.10	2.98	3.64	2.99	0.829
		4 Aug 2011	2.24	3.37	4.04	3.43	−0.495			24 Aug 2011	n/a	n/a	n/a	n/a	n/a
		22 Aug 2011	1.95	4.62	5.02	4.12	0.838			28 Aug 2011	n/a	n/a	n/a	n/a	n/a
		25 Aug 2011	0.60	3.97	4.02	3.42	0.427			9 Sep 2011	n/a	n/a	n/a	n/a	n/a
		28 Sep 2011	2.72	4.65	5.39	4.71	−0.028			11 Sep 2011	n/a	n/a	n/a	n/a	n/a
		Average	1.48	3.98	4.25	3.53	0.223			Average	0.72	4.42	4.48	2.89	0.882
IT_Col	DBF	26 Jun 2011	4.29	2.33	4.89	28.45	0.583	IT_Lav	EN L	27 Jun 2011	2.34	1.91	3.02	2.41	0.365
		8 Jul 2011	0.90	3.01	3.14	2.63	0.797			3 Jul 2011	0.69	0.81	1.06	0.82	0.895
		13 Jul 2011	0.56	2.00	2.08	1.55	0.845			9 Jul 2011	3.35	2.18	4.00	3.38	−0.494
		18 Jul 2011	2.28	3.00	3.76	3.22	0.759			11 Aug 2011	3.27	2.66	4.22	3.44	−0.030
		11 Aug 2011	3.19	3.85	5.00	3.51	0.831			12 Aug 2011	0.10	1.97	1.97	1.67	0.622
		23 Aug 2011	−1.31	3.44	3.68	3.35	0.843			20 Aug 2011	1.32	2.12	2.50	1.83	0.554
		11 Sep 2011	0.65	2.80	2.88	2.49	0.879			21 Aug 2011	1.01	1.81	2.07	1.43	0.644
		15 Sep 2011	0.83	2.61	2.73	2.35	0.897			24 Aug 2011	1.36	2.43	2.79	2.14	0.387
		16 Sep 2011	−0.12	3.01	3.02	2.83	0.886			9 Sep 2011	3.93	4.05	5.64	4.85	0.021
		17 Sep 2011	1.31	3.35	3.60	3.16	0.876			30 Sep 2011	2.73	2.97	3.21	2.78	0.789
		Average	1.26	3.36	3.59	2.95	0.820			Average	1.74	2.61	3.13	2.20	0.375
IT_Mbo	GRA	10 Apr 2011	2.99	1.14	3.20	2.99	0.257	FR_Pue	EBF	6 Apr 2011	6.10	2.22	6.49	6.10	0.646
		10 May 2011	0.47	2.65	2.69	2.33	0.612			9 Apr 2011	2.78	4.01	4.88	3.93	0.795
		25 Jun 2011	2.46	1.24	2.76	2.46	0.695			16 Apr 2011	1.21	2.07	2.39	1.73	0.877
		3 Jul 2011	3.86	1.59	4.17	3.86	0.454			17 May 2011	0.48	1.42	1.50	1.25	0.906
		24 Aug 2011	2.02	1.81	2.71	2.09	0.673			28 May 2011	4.96	1.16	5.10	4.96	0.575
		25 Aug 2011	1.17	1.41	1.83	1.54	0.767			19 Jun 2011	1.80	0.69	1.93	1.80	0.667
		13 Sep 2011	3.47	1.45	3.76	3.47	0.559			8 Jul 2011	1.27	1.57	2.02	1.65	0.861
		21 Sep 2011	0.07	1.88	1.88	1.56	0.857			14 Sep 2011	1.07	2.73	2.94	2.32	0.851
		26 Sep 2011	1.58	2.28	2.78	2.23	0.752			20 Sep 2011	2.44	3.42	4.20	2.98	0.774
		30 Sep 2011	1.13	1.61	1.97	1.55	0.820			26 Sep 2011	2.44	3.42	4.20	2.98	0.774
		Average	1.92	2.13	2.87	2.41	0.644			Average	2.66	3.15	4.12	3.07	0.773
ES_Agu	SHR	7 Apr 2011	0.21	2.79	2.20	2.49	0.891								
		27 Apr 2011	−0.65	3.00	3.07	2.76	0.744								
		8 May 2011	−0.98	3.33	3.47	2.90	0.754								
		14 May 2011	0.38	2.87	2.89	2.39	0.822								
		23 May 2011	−1.02	2.52	2.71	2.44	0.785								
		13 Jul 2011	−0.30	1.96	1.98	1.52	0.972								
		29 Jul 2011	1.13	3.72	3.88	3.16	0.587								
		14 Aug 2011	−1.30	4.67	4.85	4.49	0.817								
		26 Aug 2011	0.74	4.56	4.62	3.86	0.714								
		7 Sep 2011	2.28	2.91	3.69	2.81	0.593								
		Average	0.03	3.39	3.39	2.63	0.768								
All Sites		Average	1.40	3.29	3.69	2.81	0.641								

ESDD
6, 217–265, 2015

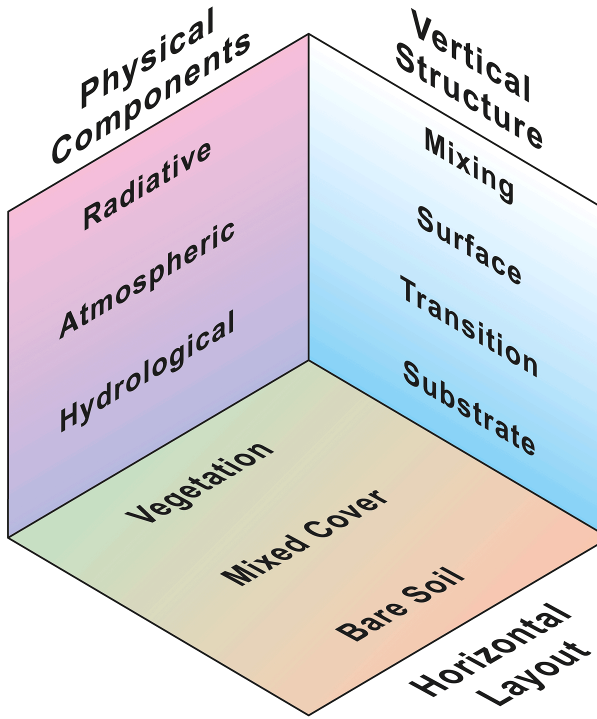

Figure 1. The three facets of SimSphere Architecture.

ESDD
6, 217–265, 2015

Appraising the capability of a land biosphere model as a tool in modelling land surface interactions

M. R. North et al.

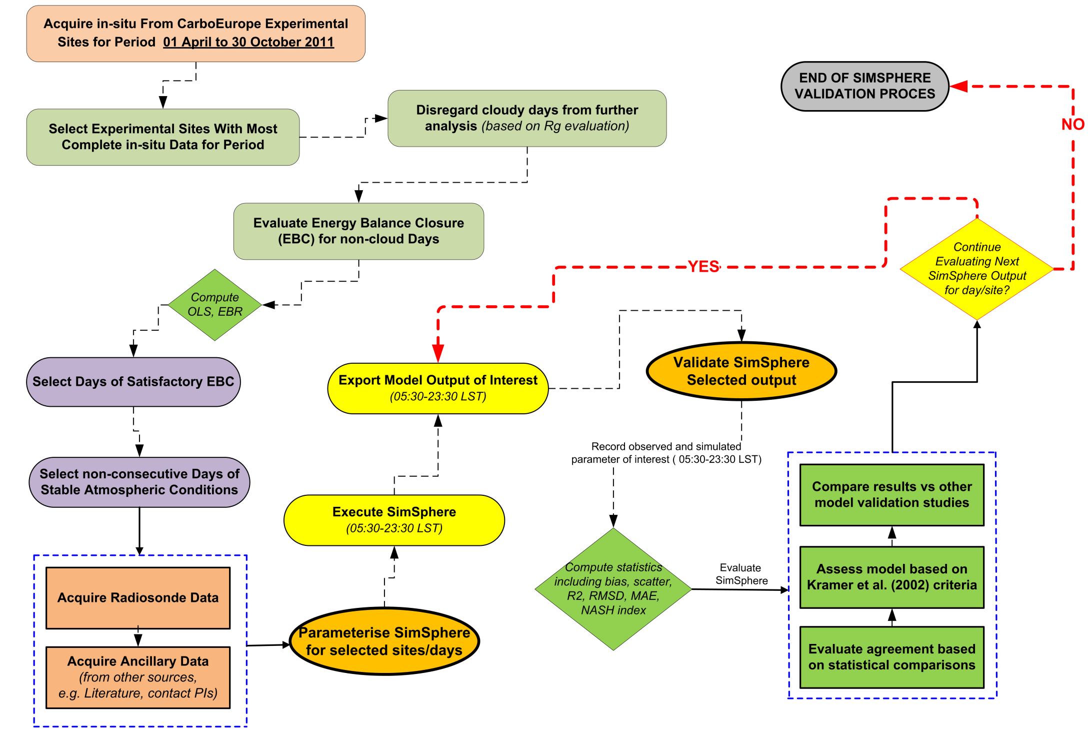

Figure 2. Overall methodology of SimSphere validation followed in this study.

ESDD
6, 217–265, 2015

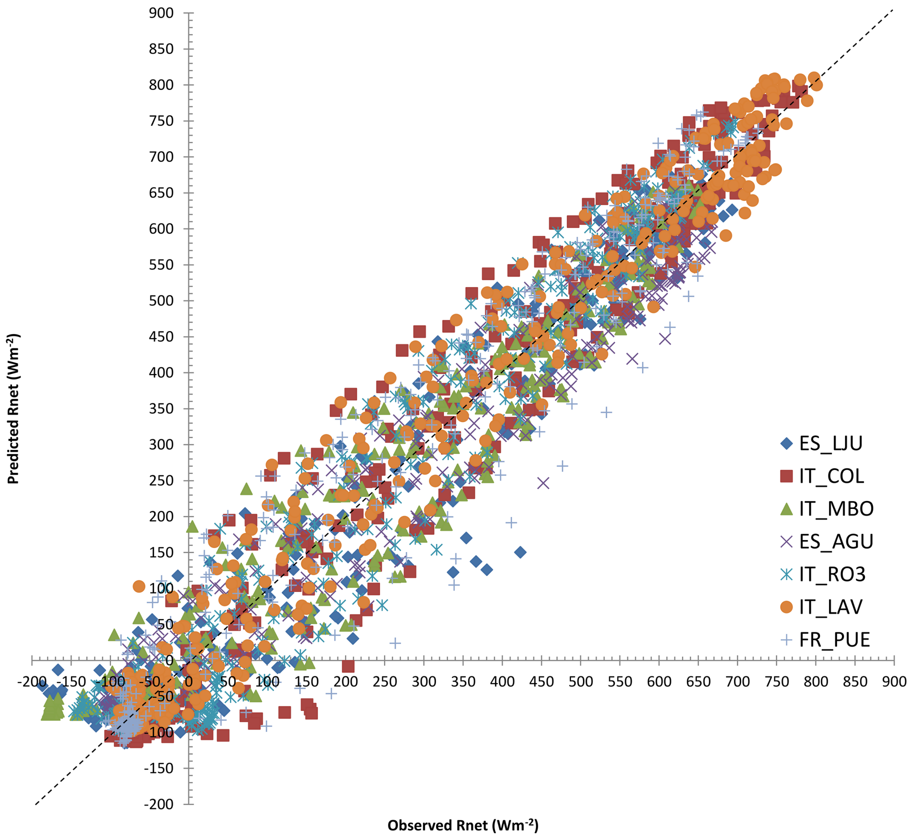

Figure 3. Scatterplot comparison of SimSphere predicted and in-situ R_{net} flux.

CC BY

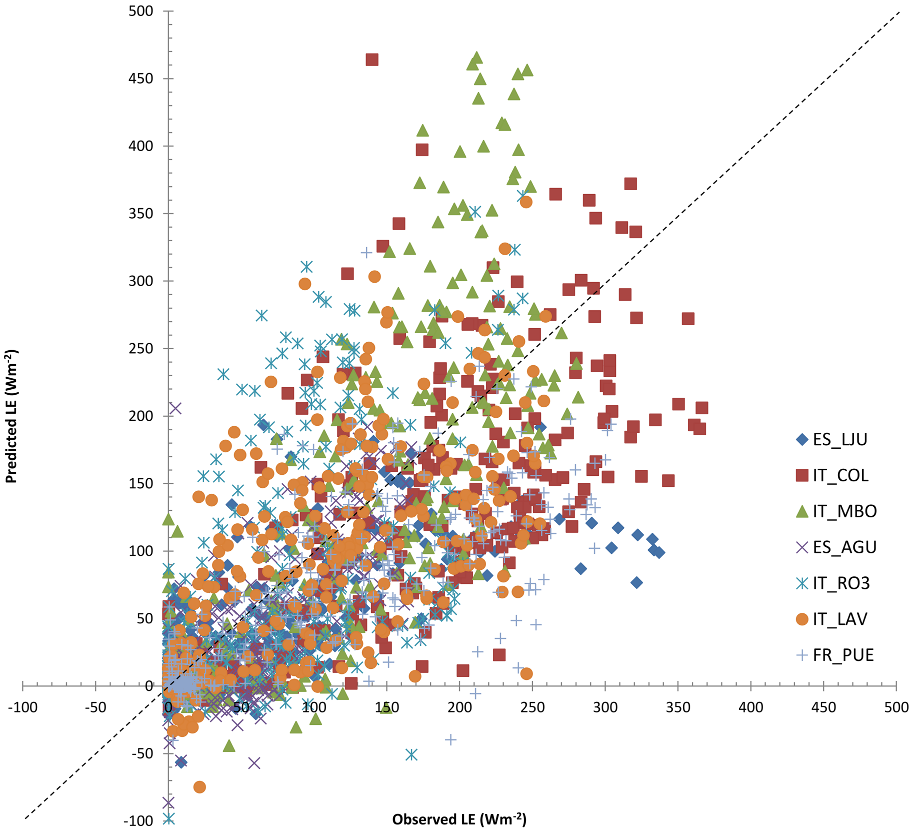

Figure 4. Scatterplot comparison of SimSphere predicted and in-situ LE flux.

ESDD
6, 217–265, 2015

Appraising the capability of a land biosphere model as a tool in modelling land surface interactions

M. R. North et al.

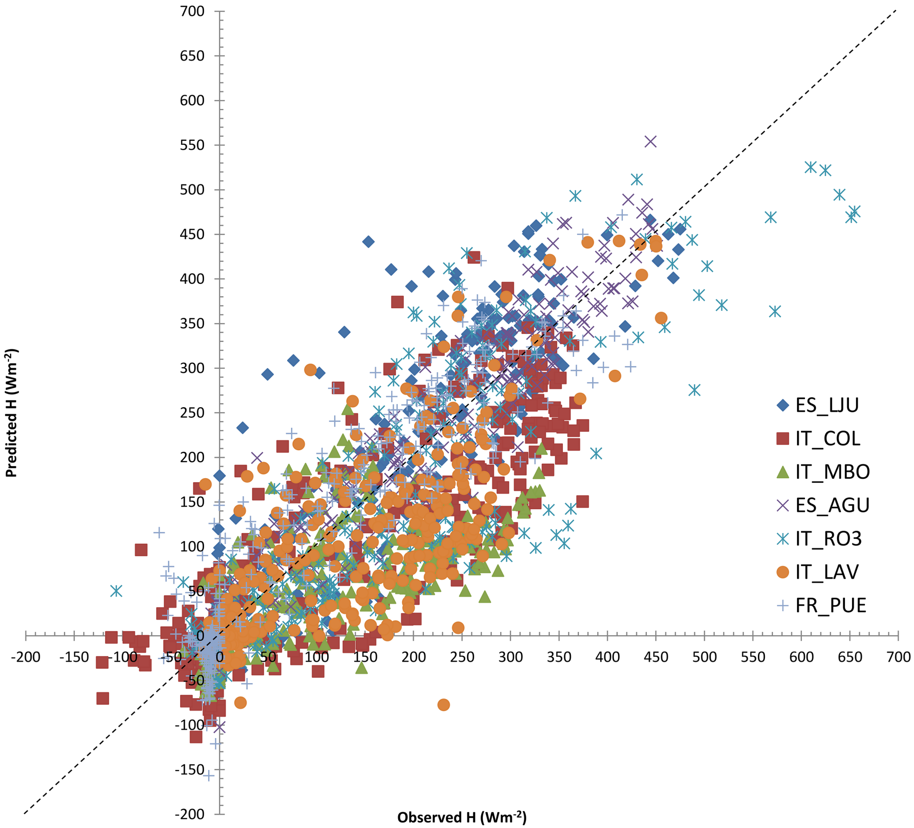

Figure 5. Scatterplot comparison of SimSphere predicted and in-situ H flux.

ESDD
6, 217–265, 2015

Appraising the capability of a land biosphere model as a tool in modelling land surface interactions

M. R. North et al.

Title Page
Abstract | Introduction
Conclusions | References
Tables | Figures
◀| |▶
◀ ▶
Back | Close
Full Screen / Esc
Printer-friendly Version
Interactive Discussion

CC BY

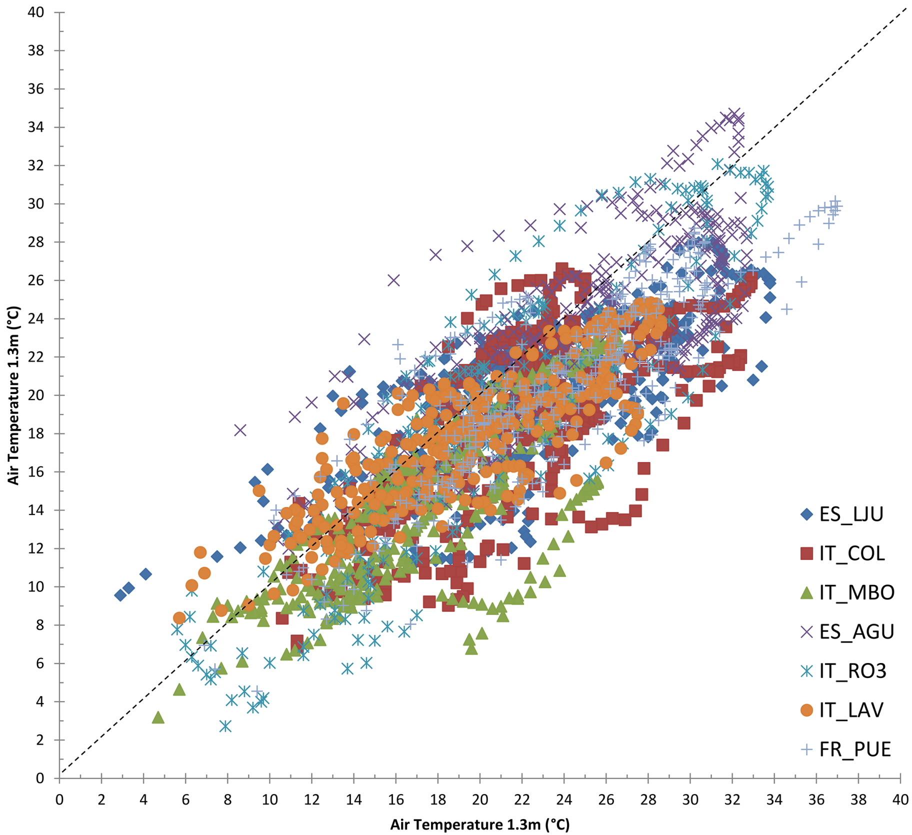

Figure 6. Scatterplot comparison of SimSphere predicted and in-situ $T_{\text{air 1.3 m}}$.

ESDD
6, 217–265, 2015

Appraising the capability of a land biosphere model as a tool in modelling land surface interactions

M. R. North et al.

Title Page
Abstract Introduction
Conclusions References
Tables Figures
◂◂ ▸▸
◂ ▸
Back Close
Full Screen / Esc
Printer-friendly Version
Interactive Discussion

CC BY

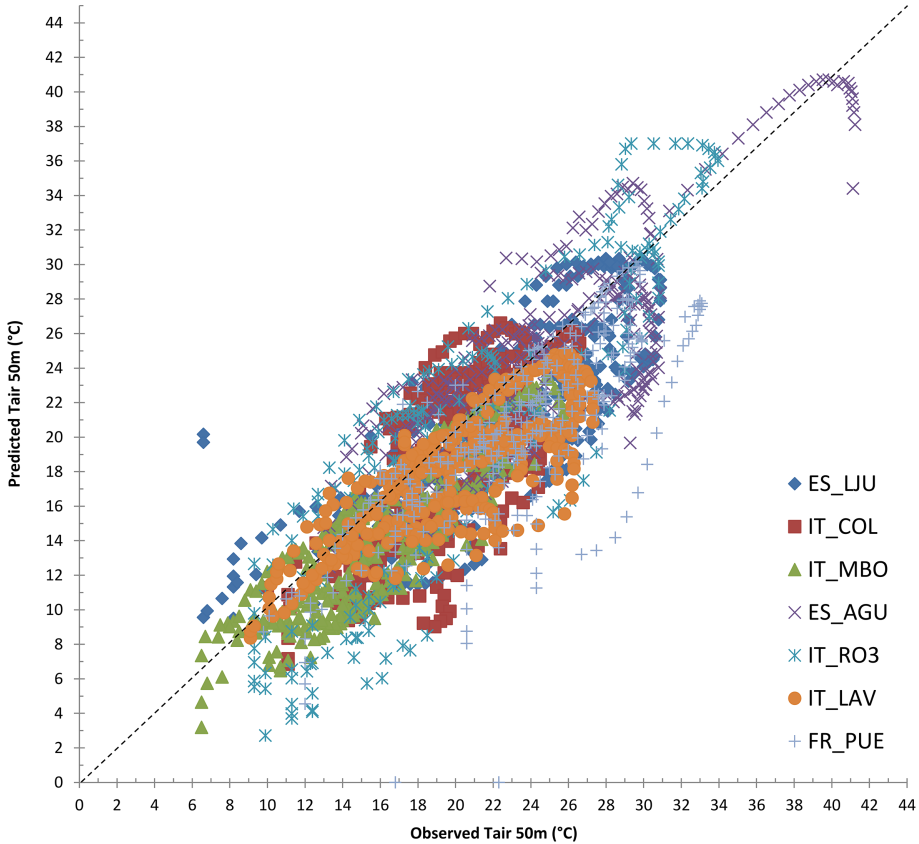

Figure 7. Scatterplot comparison of SimSphere predicted and in-situ $T_{\mathrm{air\ 50\,m}}$.

ESDD
6, 217–265, 2015

CC BY